HiNF-P to stimulate the *H4* promoter, while a Skp2 F-box mutant (Skp2ΔF, which is defective in promoting $p57^{KIP2}$ degradation) does not (data not shown). In addition, HiNF-P and/or $p220^{NPAT}$ enhanced reporter gene expression under control of multimerized HiNF-P binding sites is consistently inhibited by $p57^{KIP2}$, but not when HiNF-P elements are mutated (Fig. 5C). Taken together, our data indicate that $p57^{KIP2}$, $p27^{KIP1}$, and $p21^{CIP1/WAF1}$ exhibit differences in their ability to inhibit the $p220^{NPAT}$/HiNF-P dependent stimulation of the *histone H4* promoter (summarized in Fig. 5D). The preferential effectiveness of $p57^{KIP2}$ in blocking *H4* gene transcription is consistent with our previous observation that exogenous HiNF-P does not activate *H4* gene transcription in cell types that express high levels of endogenous $p57^{KIP2}$ (Mitra et al., 2006).

$p57^{KIP2}$ complexes with $p220^{NPAT}$

Because $p57^{KIP2}$ is more effective than $p27^{KIP1}$ or $p21^{CIP}$ in blocking HiNF-P/$p220^{NPAT}$ co-activation, we postulated that $p57^{KIP2}$ may act beyond merely inhibiting CDK2 kinase activity and have molecular specificity for $p220^{NPAT}$. Immunoprecipitation experiments reveal that $p220^{NPAT}$ forms a complex with wild type $p57^{KIP2}$ (Fig. 6). Mutants of $p220^{NPAT}$ that are defective in interactions with HiNF-P (i.e., LisH mut, LoxP1 mut) remain capable of binding to $p57^{KIP2}$. However, the $p220^{NPAT}$-ΔCDK2 mutant, which cannot be phosphorylated by CDK2 (Wei et al., 2003) and is transcriptionally inactive, does not bind to $p57^{KIP2}$ (Fig. 6A). Furthermore, the cyclin binding defective $p57^{KIP2}$-CCT mutant (Hattori et al., 2000) does not interact with $p220^{NPAT}$ (Fig. 6B, top part). Hence, CDK2

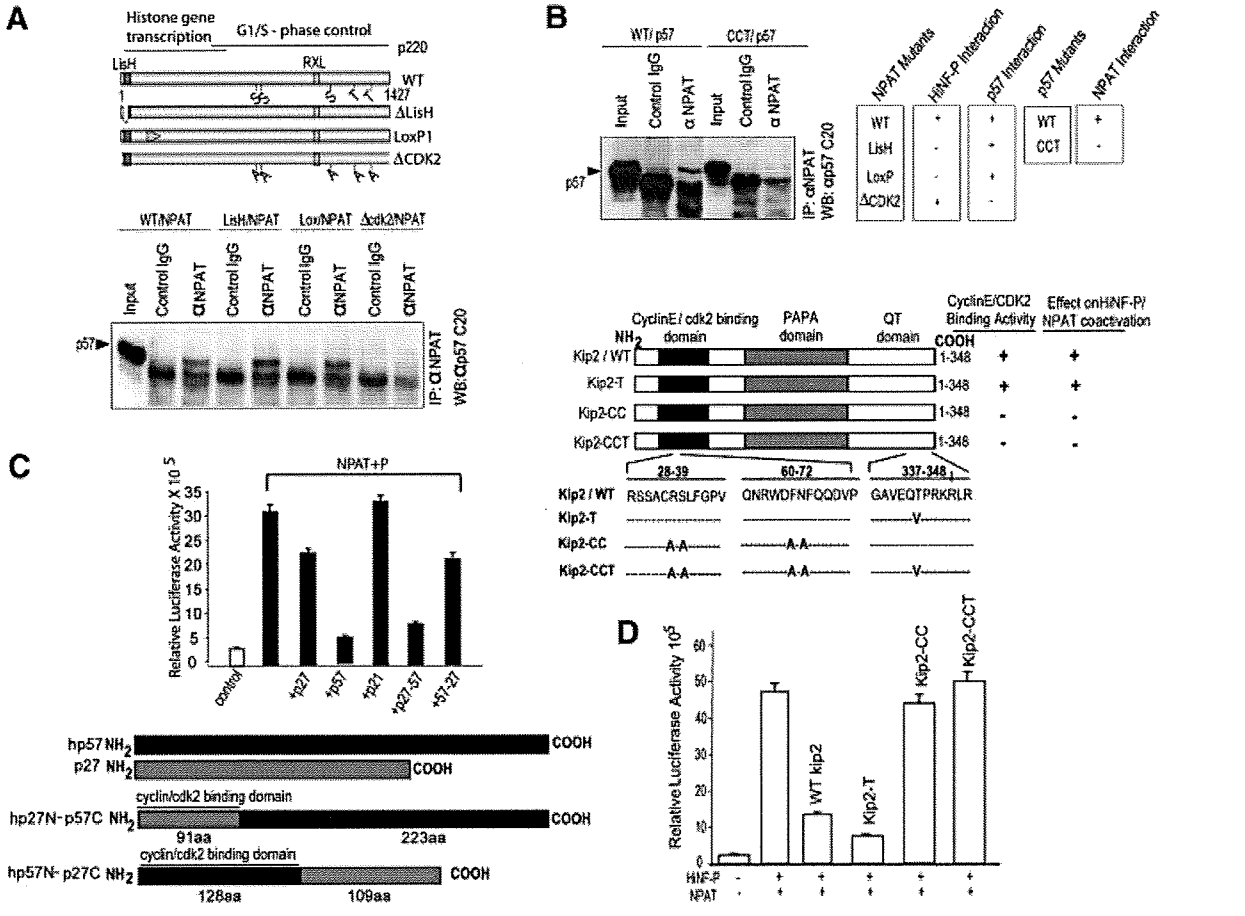

Fig. 6. $p57^{KIP2}$ and $p220^{NPAT}$ form specific complexes. A: Wild type $p220^{NPAT}$ forms a complex with $p57^{KIP2}$ via residues involved in CDK2 phosphorylation. Immuno-complexes were obtained from Cos7 cells transfected with expression vectors for $p57^{KIP2}$ (25 ng/well) and wild type or mutant $p220^{NPAT}$ proteins (200 ng/well). Whole cell protein (~100 μg) was precipitated with anti-$p220^{NPAT}$ antibody (1 μg) antibody, and analyzed by Western blotting using an anti-rabbit-$p57^{KIP2}$ antibody (1:3,000 dilution; secondary goat anti-rabbit IgG antibody = 1:5,000 dilution). Wild type $p220^{NPAT}$ and two $p220^{NPAT}$ mutants (LisH, deletion of aa 3–38; LoxP1: alanine substitutions between aa 121 and 145, respectively) interact with $p57^{KIP2}$, but the $p220^{NPAT}$-ΔCDK2 mutant with alanine substitution in five C-terminal CDK2 phosphorylation sites (S/T) does not. B: The N-terminal cyclin binding of wild type $p57^{KIP2}$ supports interactions with $p220^{NPAT}$. Wild type $p57^{KIP2}$ and a $p57^{KIP2}$ mutant with amino acid substitutions in the cyclin binding domain (see C) were expressed in Cos7 cells, and immunoprecipitates were obtained as described above (see A). Complexes with $p220^{NPAT}$ are only formed with wild type $p57^{KIP2}$ but not with $p57^{KIP2}$-CCT as indicated. The immunoprecipitation results presented here were correlated with those obtained for HiNF-P and $p220^{NPAT}$ previously (lower part). C: Inhibition of *H4* gene transcription requires the cyclin binding domain of $p57^{KIP2}$. Co-activation assays for $p220^{NPAT}$/HiNF-P were performed with cells co-transfected with vectors expressing wild type or mutant $p57^{KIP2}$ (i.e., T, CC, and CCT; 25 ng/well) and luciferase activity for each mutant is plotted. D: As in Part C, but using reciprocal in the C-termini of $p57^{KIP2}$ and $p27^{KIP1}$ are swapped.

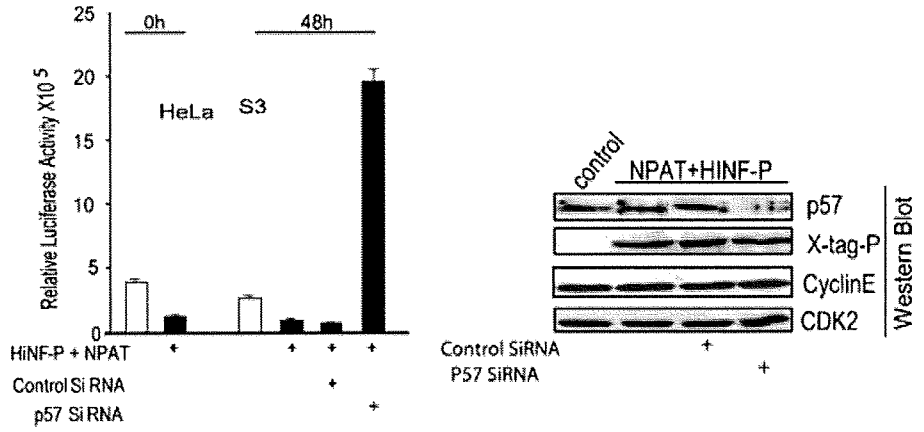

Fig. 7. Rescue of HiNF-P co-activation by $p57^{KIP2}$ siRNA and changes in endogenous *histone H4* gene expression upon $p57^{KIP2}$ modulation. Treatment of HeLa cells that express endogenous $p57^{KIP2}$ with siRNA specific for $p57^{KIP2}$ restores co-activation of HiNF-P and $p220^{NPAT}$. HeLa cells were transfected with the *H4* promoter-luciferase reporters in the presence (+) or absence of $p220^{NPAT}$ and HiNF-P expression vectors. After ~12–16 h, cells were treated with (+) control siRNA or $p57^{KIP2}$ siRNA (100 nM). Luciferase activity was measured after 48 h. Selective siRNA mediated deficiency of $p57^{KIP2}$ relative to Cyclin E, CDK2 and HiNF-P was confirmed by immunoblotting.

phosphorylatable amino acids in the C-terminal half of $p220^{NPAT}$ and the N-terminal cyclin binding domain of $p57^{KIP2}$ both contribute to the $p220^{NPAT}/p57^{KIP2}$ interaction.

We examined which functions of $p57^{KIP2}$ are required to neutralize co-activation of the HiNF-P/$p220^{NPAT}$ complex (Fig. 6C). Cyclin binding domain mutants of $p57^{KIP2}$ (CC and CCT) do not block enhancement by HiNF-P and $p220^{NPAT}$ in reporter gene assays. However, the $p57^{KIP2}$-T mutant that is defective for Skp2 dependent degradation (Hattori et al., 2000) effectively blocks promoter co-stimulation by HiNF-P and $p220^{NPAT}$. Hence, functional inhibition of $p220^{NPAT}$ correlates with the abilities of $p57^{KIP2}$ to block CDK2 activity through a cyclin/CDK interaction, to participate in a complex with $p220^{NPAT}$, and to prevent phosphorylation of both T1270 and T1350 of $p220^{NPAT}$.

We also investigated the role of the unique C-terminus of $p57^{KIP2}$ by analyzing the functional effects of $p27^{KIP1}$-$p57^{KIP2}$ and $p57^{KIP2}$-$p27^{KIP1}$ chimeras on *H4* gene transcription (Fig. 6D). The $p27^{KIP1}$-$p57^{KIP2}$ chimera is as effective as wild type $p57^{KIP2}$ in blocking the activation of *H4* gene transcription by $p220^{NPAT}$ and HiNF-P, while neither the $p57^{KIP2}$-$p27^{KIP1}$ chimera nor wild type $p27^{KIP1}$ is inhibitory at the concentrations we tested. Hence, the cyclin binding function and the C-terminus of $p57^{KIP2}$ are both necessary for inhibiting histone gene transcription.

Modulation of $p57^{KIP2}$ levels alters the co-activation potential of HiNF-P/$p220^{NPAT}$ and *Histone H4* gene expression

Exogenous HiNF-P does not activate *H4* gene transcription in cells that express high levels of endogenous $p57^{KIP2}$ (Mitra et al., 2006), perhaps because of the formation of inactive complexes containing HiNF-P, $p220^{NPAT}$, $p57^{KIP2}$ and perhaps other components (see Discussion Section). Therefore, we assessed whether removal of endogenous $p57^{KIP2}$ would alter the activity of HiNF-P and/or $p220^{NPAT}$ and convert HiNF-P/$p220^{NPAT}$ complexes into functional activators of *H4* gene transcription. The results show that treatment with $p57^{KIP2}$ siRNA reduces endogenous $p57^{KIP2}$ mRNA and increases *histone H4* gene expression in HeLa S3 cells, suggesting that $p57^{KIP2}$ may control the co-activation potential of HiNF-P and $p220^{NPAT}$ (Fig. 7).

Inhibition of $p220^{NPAT}$/HiNF-P co-activation by $p57^{KIP2}$ in normal diploid cells

Because the above studies were performed with tumor-derived cell lines, the question arises whether $p57^{KIP2}$ suppresses *histone H4* gene expression or activation of the *histone H4* gene promoter by the $p220^{NPAT}$/HiNF-P complex in cells with normal cell growth characteristics. In one set of experiments, we examined expression of several representative mouse *histone H4* genes in embryonic fibroblasts from wild type mice and mice with heterozygous or homozygous null mutations in the mouse $p57^{Kip2}$ gene (Fig. 8A). The results show that loss of either one or two $p57^{Kip2}$ alleles abolishes $p57^{Kip2}$ gene expression as expected, with modest compensatory changes in the expression of $p21^{Cip/Waf}$. However, we did not observe changes in the expression of the three mouse *histone H4* genes we examined nor in the expression of mRNAs for *HiNF-P* or *HPRT*. Hence, loss of $p57^{Kip2}$ mRNA expression does not alter the accumulation of *histone H4* mRNAs. This finding is consistent with results presented in Figure 1 that reveal that diminished *histone H4* gene transcription is not necessarily reflected by a change in histone mRNA levels (e.g., due to simultaneous changes in histone mRNA stability). We performed nuclear run-on analysis with MEFs with heterozygous or homozygous null mutations in $p57^{Kip2}$ to test whether loss of this CKI changes *histone H4* gene transcription. However, the experimental variation in cell growth rates of different MEF preparations appeared to dominate the outcome and we were not able to ascertain genotype-specific changes in transcription rates using this approach (data not shown).

In a final set of experiments, we studied the effect of $p57^{KIP2}$ protein on a human *histone H4* gene promoter construct in normal diploid human fibroblasts (WI38 cells) (Fig. 8B). The results show that $p57^{KIP2}$ suppresses *histone H4* gene promoter activation by $p220^{NPAT}$ and HiNF-P. We conclude that $p57^{KIP2}$ can control the transcriptional output of the Cyclin E/CDK2/$p220^{NPAT}$/HiNF-P signaling pathway, but this regulatory level does not immediately influence accumulation of *histone H4* mRNAs.

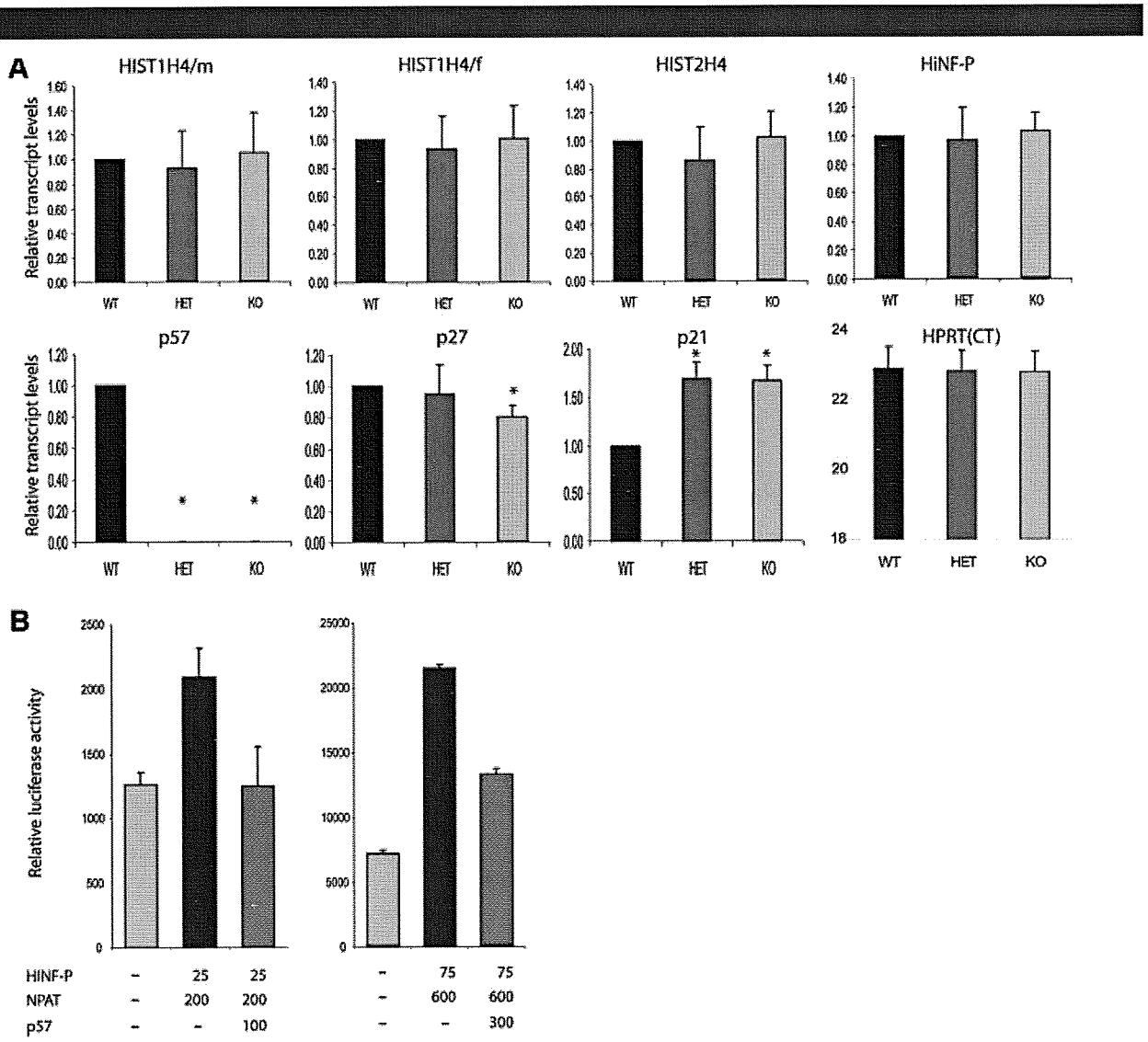

Fig. 8. p57^{Kip2} suppresses *histone H4* promoter activity in normal diploid human cells. A: Total RNA from wild type *p57* (WT), heterozygous *p57* null (HET) and homozygous *p57* null (KO) mouse embryonic fibroblasts was examined for mRNA expression of mouse *HiNF-P*, *Hist2H4*, *HistH4/m*, *Hist1H4/f*, *p57*, *p27*, and *p21* using quantitative RT-PCR. Values were calculated with the ΔΔCT method using *HPRT* as an internal control. We did not observe significant changes in the expression of *Hist2H4*, *Hist1H4/m*, and *Hist1H4/f histone* in HET and KO cells compared to WT cells. As expected *p57* mRNA is absent in KO and HET cells (HET cells are functionally null for *p57* due to imprinting), while expression of *p21* mRNA in KO and HET cells is significantly higher than in WT cells. Student's t-test (unpaired, two-tailed, non-parametric) was used to calculate significance by comparing gene expression in WT to either HET or KO cells. Asterisks (*) indicate *P*-values < 0.05. B: WI-38 human diploid fibroblasts were plated at a density of 1.6 × 10^5/well in six-well plates and transiently transfected at day 2 after plating at a cell density of ~30% with wild-type *histone H4* promoter luciferase reporter construct. Cells were co-transfected with the indicated amounts of expression vectors for HiNF-P (P), p220^{NPAT} (N) and p57, or an empty vector (EV). Experiments were performed with either 200 ng (left graph) or 600 ng (right graph) of firefly luciferase reporter gene construct. The promoterless *Renilla* luciferase control plasmid was also different (25 ng, left graph; 75 ng, right graph), but total amount of DNA was maintained at 2.5 μg in every transfection.

Discussion

The cyclin E/CDK2 dependent phosphorylation of pRB and p220^{NPAT} ensures that E2F and HiNF-P can activate their respective target genes, thus mechanistically separating the onset of histone production from DNA replication at the G1/S phase transition (Fig. 9). Release of E2F from pRB can be inhibited by p57^{KIP2}, p27^{KIP1} or p21$^{CIP1/WAF1}$ with each preventing phosphorylation of pRB by blocking the activity of CDK2/Cyclin E kinase (Sherr and Roberts, 2004). Our study shows that activity of the p220^{NPAT}/HiNF-P transcriptional co-activation complex is also directly controlled by CKIs. CKIs prevent phosphorylation by CDK2 of at least two phospho-epitopes of p220^{NPAT} that stimulate the functional activity of the p220^{NPAT}/HiNF-P complex. However, our studies suggest that p57^{KIP2} is more potent than p27^{KIP1} or p21$^{CIP1/WAF1}$ in blocking the in situ phosphorylation of p220^{NPAT} at Cajal Body-related subnuclear foci.

Interestingly, p57^{KIP2} has weaker intrinsic CDK2 inhibitory activity than p27^{KIP1} and our data suggest p57^{KIP2} may compensate for weaker CDK2 inhibition by forming a complex with its substrate p220^{NPAT}. The question arises how p57^{KIP2} but not p27^{KIP1} or p21$^{CIP/WAF1}$ can selectively recognize p220^{NPAT}. The C-terminal sequences (e.g., PAPA repeats) of p57^{KIP2} differ from the other two CKIs (p27^{KIP1} and p21$^{CIP1/WAF1}$), and a chimeric protein that contains the

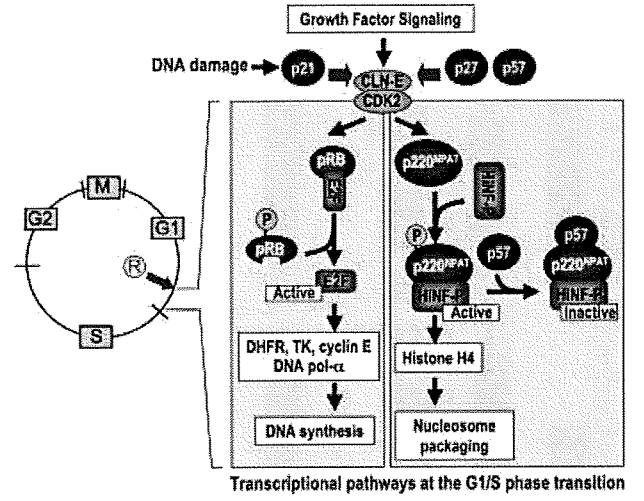

Fig. 9. Control of the HiNF-P/p220^{NPAT} pathway by p57^{KIP2}. *Histone H4* gene transcription is controlled by the HiNF-P/ p220^{NPAT} complex that is activated in parallel to the E2F/pRB pathway that controls transcription of genes involved in nucleotide metabolism and DNA synthesis. Both pathways are responsive to growth factor dependent induction of CDK2/cyclin E at the R-point, and thus sensitive to the levels of CDK inhibitors. The findings in this study suggest that while p57^{KIP2} is not a strong CDK inhibitor, it can effectively inhibit CDK phosphorylation of p220^{NPAT} through direct protein/protein interactions. It is possible that p57^{KIP2} can be recruited to histone gene promoters through interaction with the HiNF-P/ p220^{NPAT} complex.

C-terminus of p57^{KIP2} fused to the cyclin binding domain of p27^{KIP1} is as effective as the wild type p57^{KIP2} protein in blocking p220^{NPAT}/HiNF-P activity. The unique structure of p57^{KIP2} may provide the requisite specificity for direct interactions with p220^{NPAT} and thus endow p57^{KIP2} with its ability to suppress the function of p220^{NPAT} more effectively. However, CKIs are unstructured in solution when they do not interact with their cognate cyclin/CDK complexes (Adkins and Lumb, 2002; Lacy et al., 2004). Therefore, it is conceivable that p57^{KIP2} may interact with p220^{NPAT} through a cyclin/CDK protein bridge with the unique C-terminus of p57^{KIP2} stabilizing the ternary complex. Interestingly, both p57^{KIP2} and p220^{NPAT} are CDK2 substrates and contain cyclin binding motifs which could permit formation of larger complexes and/or an exchange of components (e.g., cyclin E or CDK2). Consistent with this model, the cyclin binding motif and unique C-terminus of p57^{KIP2}, as well as the CDK2 phosphorylation sites of p220^{NPAT}, are each required for the formation of complexes containing these two proteins.

It remains to be established whether the regulation of the p220^{NPAT}/HiNF-P complex occurs only at the level of protein/protein interactions or may also reflect promoter recruitment. We have been unable to detect p57 on the *H4* gene promoter, possibly for technical reasons (e.g., detection of promoter-bound p57 may require multiple protein/DNA and protein/protein cross-links). Similarly, it will be of future interest to examine whether phosphorylation of p220^{NPAT} at the T1270 and T1350 phospho-epitopes affects recruitment of p220^{NPAT} to the *H4* promoter. However, it is clear from our previous studies (Miele et al., 2005; Holmes et al., 2005; Mitra et al., 2007) that recruitment of both HiNF-P and p220^{NPAT} to *histone H4* gene promoters is detected in both T98G cells where p57 levels are below the level of detection, and in HeLa cells that express robust levels of p57. Thus, it appears that recruitment of HiNF-P and p220^{NPAT} to *H4* gene promoters is independent of p57^{KIP2}.

We have previously shown that exogenous HiNF-P cannot activate *H4* gene transcription if endogenous levels of p57^{KIP2} are high (Mitra et al., 2006). Consistent with these findings, the data presented here indicate that p57^{KIP2} is the most effective CKI in suppressing gene activation by the p220^{NPAT}/HiNF-P complex and operates via the HiNF-P binding motif in the cell cycle domain of *histone H4* gene promoters. Furthermore, Skp2-dependent degradation and siRNA induced deficiency of p57^{KIP2} can each alleviate inhibition of the p220^{NPAT}/HiNF-P pathway in cells that express p57^{KIP2}. Depletion of p57^{KIP2} levels by siRNA also alters the relative expression of different *histone H4* gene copies. Taken together, we propose that one of the biological functions of p57^{KIP2} in vivo is to control the activity of p220^{NPAT} as a co-activator of the HiNF-P mediated stimulation of *histone H4* gene promoter activity.

The greater effectiveness of p57^{KIP2} to block the function of the HiNF-P/p220^{NPAT} complex on the *H4* gene promoter is consistent with cell type specific differences in the expression of this CKI in relation to the other two CKI members. For example, during myoblast differentiation, p57^{KIP2} is upregulated in parallel with p21$^{CIP1/WAF1}$, while p57^{KIP2} and p27^{KIP1} are selectively expressed in differentiated osteoblasts (Drissi et al., 1999; Urano et al., 1999). In both mesenchymal lineages, the elevated expression of p57^{KIP2} will support efficient inhibition of *histone H4* gene transcription at the onset of quiescence during differentiation. However, the majority of proliferating cells express p57^{KIP2} only at very low levels and its function in blocking *histone H4* gene expression may be mostly restricted to quiescent cells. In comparison, the physiological elevation of p21$^{CIP1/WAF1}$ during the DNA damage response in proliferating cells may preferentially permit continued signaling through the CDK2 responsive p220^{NPAT}/HiNF-P pathway but not the E2F/RB pathway to allow histone gene transcription during DNA repair.

Acknowledgments

We thank the members of our laboratories for stimulating discussions, as well as Andy Koff (Sloan Kettering Institute, New York, NY) and Gerard Zambetti (St. Jude Children's Hospital, Memphis, TN) for critical evaluation of this manuscript. The contents of this manuscript are solely the responsibility of the authors and do not necessarily represent the official views of the National Institutes of Health.

Literature Cited

Adkins JN, Lumb KJ. 2002. Intrinsic structural disorder and sequence features of the cell cycle inhibitor p57Kip2. Proteins 46:1–7.

Baumbach LL, Stein GS, Stein JL. 1987. Regulation of human histone gene expression: Transcriptional and posttranscriptional control in the coupling of histone messenger RNA stability with DNA replication. Biochemistry 26:6178–6187.

Becker KA, Ghule PN, Therrien JA, Lian JB, Stein JL, van Wijnen AJ, Stein GS. 2006. Self-renewal of human embryonic stem cells is supported by a shortened G1 cell cycle phase. J Cell Physiol 209:883–893.

Becker KA, Stein JL, Lian JB, van Wijnen AJ, Stein GS. 2007. Establishment of histone gene regulation and cell cycle checkpoint control in human embryonic stem cells. J Cell Physiol 210:517–526.

Blagosklonny MV, Pardee AB. 2002. The restriction point of the cell cycle. Cell Cycle 1:103–110.

Canalli AA, Yang H, Jeha S, Hoshino K, Sanchez-Gonzalez B, Brandt M, Pierce S, Kantarjian H, Issa JP, Garcia-Manero G. 2005. Aberrant DNA methylation of a cell cycle regulatory pathway composed of P73, P15 and P57KIP2 is a rare event in children with acute lymphocytic leukemia. Leuk Res 29:881–885.

Caspary T, Cleary MA, Perlman EJ, Zhang P, Elledge SJ, Tilghman SM. 1999. Oppositely imprinted genes p57(Kip2) and igf2 interact in a mouse model for Beckwith-Wiedemann syndrome. Genes Dev 13:3115–3124.

Drissi H, Hushka D, Aslam F, Nguyen Q, Buffone E, Koff A, van Wijnen A, Lian JB, Stein JL, Stein GS. 1999. The cell cycle regulator p27kip1 contributes to growth and differentiation of osteoblasts. Cancer Res 59:3705–3711.

Dyson N. 1998. The regulation of E2F by pRB-family proteins. Genes Dev 12:2245–2262.

el-Deiry WS, Harper JW, O'Connor PM, Velculescu VE, Canman CE, Jackman J, Pietenpol JA, Burrell M, Hill DE, Wang Y. 1994. WAF1/CIP1 is induced in p53-mediated G1 arrest and apoptosis. Cancer Res 54:1169–1174.

Ghule PN, Becker KA, Harper JW, Lian JB, Stein JL, van Wijnen AJ, Stein GS. 2007. Cell cycle dependent phosphorylation and subnuclear organization of the histone gene regulator $p220^{NPAT}$ in human embryonic stem cells. J Cell Physiol 213:9–17.

Harper JW, Adami GR, Wei N, Keyomarsi K, Elledge SJ. 1993. The p21 Cdk-interacting protein Cip1 is a potent inhibitor of G1 cyclin-dependent kinases. Cell 75:805–816.

Hattori N, Davies TC, nson-Cartwright L, Cross JC. 2000. Periodic expression of the cyclin-dependent kinase inhibitor p57(Kip2) in trophoblast giant cells defines a G2-like gap phase of the endocycle. Mol Biol Cell 11:1037–1045.

Holmes WF, Braastad CD, Mitra P, Hampe C, Doenecke D, Albig W, Stein JL, van Wijnen AJ, Stein GS. 2005. Coordinate control and selective expression of the full complement of replication-dependent histone H4 genes in normal and cancer cells. J Biol Chem 280:37400–37407.

Kamura T, Hara T, Kotoshiba S, Yada M, Ishida N, Imaki H, Hatakeyama S, Nakayama K, Nakayama KI. 2003. Degradation of p57Kip2 mediated by SCFSkp2-dependent ubiquitylation. Proc Natl Acad Sci USA 100:10231–10236.

Kikuchi T, Toyota M, Itoh F, Suzuki H, Obata T, Yamamoto H, Kakiuchi H, Kusano M, Issa JP, Tokino T, Imai K. 2002. Inactivation of p57KIP2 by regional promoter hypermethylation and histone deacetylation in human tumors. Oncogene 21:2741–2749.

Kondo M, Matsuoka S, Uchida K, Osada H, Nagatake M, Takagi K, Harper JW, Takahashi T, Elledge SJ, Takahashi T. 1996. Selective maternal-allele loss in human lung cancers of the maternally expressed p57KIP2 gene at 11p15.5. Oncogene 12:1365–1368.

Lacy ER, Filippov I, Lewis WS, Otieno S, Xiao L, Weiss S, Hengst L, Kriwacki RW. 2004. p27 binds cyclin-CDK complexes through a sequential mechanism involving binding-induced protein folding. Nat Struct Mol Biol 11:358–364.

Li Y, Nagai H, Ohno T, Yuge M, Hatano S, Ito E, Mori N, Saito H, Kinoshita T. 2002. Aberrant DNA methylation of p57(KIP2) gene in the promoter region in lymphoid malignancies of B-cell phenotype. Blood 100:2572–2577.

Lodygin D, Epanchintsev A, Menssen A, Diebold J, Hermeking H. 2005. Functional epigenomics identifies genes frequently silenced in prostate cancer. Cancer Res 65:4218–4227.

Luo Y, Hurwitz J, Massague J. 1995. Cell-cycle inhibition by independent CDK and PCNA binding domains in p21Cip1. Nature 375:159–161.

Ma T, Van Tine BA, Wei Y, Garrett MD, Nelson D, Adams PD, Wang J, Qin J, Chow LT, Harper JW. 2000. Cell cycle-regulated phosphorylation of p220(NPAT) by cyclin E/Cdk2 in Cajal bodies promotes histone gene transcription. Genes Dev 14:2298–2313.

Matsuoka S, Edwards MC, Bai C, Parker S, Zhang P, Baldini A, Harper JW, Elledge SJ. 1995. p57KIP2, a structurally distinct member of the p21CIP1 Cdk inhibitor family, is a candidate tumor suppressor gene. Genes Dev 9:650–662.

Matsuoka S, Thompson JS, Edwards MC, Bartletta JM, Grundy P, Kalikin LM, Harper JW, Elledge SJ, Feinberg AP. 1996. Imprinting of the gene encoding a human cyclin-dependent kinase inhibitor, p57KIP2, on chromosome 11p15. Proc Natl Acad Sci USA 93:3026–3030.

Medina R, van Wijnen AJ, Stein GS, Stein JL. 2006. The histone gene transcription factor HiNF-P stabilizes its cell cycle regulatory co-activator $p220^{NPAT}$. Biochemistry 45:15915–15920.

Medina R, van der Deen M, Miele-Chamberland A, Xie RL, van Wijnen AJ, Stein JL, Stein GS. 2007. The HiNF-P/$p220^{NPAT}$ cell cycle signaling pathway controls non-histone target genes. Cancer Res 67:10334–10342.

Miele A, Braastad CD, Holmes WF, Mitra P, Medina R, Xie R, Zaidi SK, Ye X, Wei Y, Harper JW, van Wijnen AJ, Stein JL, Stein GS. 2005. HiNF-P directly links the cyclin E/CDK1/$p220^{NPAT}$ pathway to histone H4 gene regulation at the G1/S phase cell cycle transition. Mol Cell Biol 25:6140–6153.

Miele A, Medina R, van Wijnen AJ, Stein GS, Stein JL. 2007. The interactome of the histone gene regulatory factor HiNF-P suggests novel cell cycle related roles in transcriptional control and RNA processing. J Cell Biochem 102:136–148.

Mitra P, Xie RL, Medina R, Hovhannisyan H, Zaidi SK, Wei Y, Harper JW, Stein JL, van Wijnen AJ, Stein GS. 2003. Identification of HiNF-P, a key activator of cell cycle controlled histone H4 genes at the onset of S phase. Mol Cell Biol 23:8110–8123.

Mitra P, Xie R, Harper JW, Stein JL, Stein GS, van Wijnen AJ. 2006. HiNF-P is a bifunctional regulator of cell cycle controlled histone H4 gene transcription.

Mitra P, Xie R, Harper JW, Stein JL, Stein GS, van Wijnen AJ. 2007. HiNF-P is a bifunctional regulator of cell cycle controlled histone H4 gene transcription. J Cell Biochem 101:181–191.

Nakayama K, Nakayama K. 1998. Cip/Kip cyclin-dependent kinase inhibitors: Brakes of the cell cycle engine during development. BioEssays 20:1020–1029.

Nevins JR. 2001. The Rb/E2F pathway and cancer. Hum Mol Genet 10:699–703.

Pauli U, Chrysogelos S, Stein G, Stein J, Nick H. 1987. Protein-DNA interactions in vivo upstream of a cell cycle- regulated human H4 histone gene. Science 236: 1308–1311.

Reynaud EG, Pelpel K, Guillier M, Leibovitch MP, Leibovitch SA. 1999. p57(Kip2) stabilizes the MyoD protein by inhibiting cyclin E-Cdk2 kinase activity in growing myoblasts. Mol Cell Biol 19:7621–7629.

Sherr CJ, Roberts JM. 1999. CDK inhibitors: Positive and negative regulators of G1-phase progression. Genes Dev 13:1501–1512.

Sherr CJ, Roberts JM. 2004. Living with or without cyclins and cyclin-dependent kinases. Genes Dev 18:2699–2711.

Shopland LS, Byron M, Stein JL, Lian JB, Stein GS, Lawrence JB. 2001. Replication-dependent histone gene expression is related to Cajal body (CB) association but does not require sustained CB contact. Mol Biol Cell 12:565–576.

Stein GS, Stein JL, van Wijnen AJ, Lian JB. 1992. Regulation of histone gene expression. Curr Opin Cell Biol 4:166–173.

Urano T, Yashiroda H, Muraoka M, Tanaka K, Hosoi T, Inoue S, Ouchi Y, Toyoshima H. 1999. $p57^{Kip2}$ is degraded through the proteasome in osteoblasts stimulated to proliferation by transforming growth factor β1. J Biol Chem 274:12197–12200.

van Wijnen AJ, van den Ent FM, Lian JB, Stein JL, Stein GS. 1992. Overlapping and CpG methylation-sensitive protein-DNA interactions at the histone H4 transcriptional cell cycle domain: Distinctions between two human H4 gene promoters. Mol Cell Biol 12:3273–3287.

Wei Y, Jin J, Harper JW. 2003. The cyclin E/Cdk2 substrate and Cajal body component p220(NPAT) activates histone transcription through a novel LisH-like domain. Mol Cell Biol 23:3669–3680.

Xie RL, Liu L, Mitra P, Stein JL, van Wijnen AJ, Stein GS. 2007. Transcriptional activation of the histone nuclear factor P (HiNF-P) gene by HiNF-P and its cyclin E/CDK2 responsive co-factor p220(NPAT) defines a novel autoregulatory loop at the G1/S phase transition. Gene 402:94–102.

Zhang P, Liégeois NJ, Wong C, Finegold M, Hou H, Thompson JC, Silverman A, Harper JW, DePinho RA, Elledge SJ. 1997. Altered cell differentiation and proliferation in mice lacking $p57^{KIP2}$ indicates a role in Beckwith-Wiedemann syndrome. Nature 387:151–158.

Zhang P, Wong C, DePinho RA, Harper JW, Elledge SJ. 1998. Cooperation between the Cdk inhibitors $p27^{Kip1}$ and $p57^{KIP2}$ in the control of tissue growth and development. Genes Dev 12:3162–3167.

Zhang P, Wong C, Liu D, Finegold M, Harper JW, Elledge SJ. 1999. $p21^{CIP1}$ and $p57^{KIP2}$ control muscle differentiation at the myogenin step. Genes Dev 13:213–224.

Zhao J, Kennedy BK, Lawrence BD, Barbie DA, Matera AG, Fletcher JA, Harlow E. 2000. NPAT links cyclin E-Cdk2 to the regulation of replication-dependent histone gene transcription. Genes Dev 14:2283–2297.

MOLECULAR AND CELLULAR BIOLOGY, Sept. 2009, p. 5104–5114 Vol. 29, No. 18
0270-7306/09/$08.00+0 doi:10.1128/MCB.00465-09

Mechanoregulation of Proliferation▽

Xiaogang Jiang,[1]† Paul F. Austin,[1] Robert A. Niederhoff,[1] Scott R. Manson,[1] Jacob J. Riehm,[1] Brian L. Cook,[1]‡ Gina Pengue,[1] Kanchan Chitaley,[3] Keiko Nakayama,[4] Keiichi I. Nakayama,[5] and Steven J. Weintraub[1,2]*

Division of Urology and Alvin J. Siteman Cancer Center, Washington University School of Medicine, St. Louis, Missouri 63110[1]; Department of Internal Medicine, St. Louis VA Medical Center, John Cochran Division, 915 North Grand Blvd., St. Louis, Missouri 63106[2]; Department of Urology, University of Washington, Box 358050, 815 Mercer Street, Seattle, Washington 98109[3]; Center for Translational and Advanced Animal Research on Human Diseases, Tohoku University School of Medicine, Sendai, Japan[4]; and Department of Molecular and Cellular Biology, Medical Institute of Bioregulation Kyushu University, Fukuoka, Japan[5]

Received 9 April 2009/Returned for modification 26 May 2009/Accepted 30 June 2009

The proliferation of all nontransformed adherent cells is dependent upon the development of mechanical tension within the cell; however, little is known about the mechanisms by which signals regulated by mechanical tension are integrated with those regulated by growth factors. We show here that Skp2, a component of a ubiquitin ligase complex that mediates the degradation of several proteins that inhibit proliferation, is upregulated when increased mechanical tension develops in intact smooth muscle and that its upregulation is critical for the smooth muscle proliferative response to increased mechanical tension. Notably, whereas growth factors regulate Skp2 at the level of protein stability, we found that mechanical tension regulates Skp2 at the transcriptional level. Importantly, we demonstrate that the calcium-regulated transcription factor NFATc1 is a critical mediator of the effect of increased mechanical tension on Skp2 transcription. These findings identify Skp2 as a node at which signals from mechanical tension and growth factors are integrated to regulate proliferation, and they define calcium-NFAT-Skp2 signaling as a critical pathway in the mechanoregulation of proliferation.

Cellular proliferation is regulated by (i) soluble factors, (ii) adhesion to the extracellular matrix, and (iii) the mechanical tension within the cytoskeleton. Although most studies of the regulation of proliferation have focused on the role of soluble factors and adhesion, it is clear that the role of the mechanical tension within the cytoskeleton is of equal importance. In fact, the proliferation of all nontransformed adherent cells is dependent upon the development of mechanical tension (21).

The level of mechanical tension within the cytoskeleton is determined by three factors: (i) the tractional force generated by the cytoskeleton, (ii) the compliance of the extracellular matrix, and (iii) any pulling force transmitted through the extracellular matrix to the cell. These three factors are likely to have a critical regulatory role in every nonhematologic process in which proliferation occurs. Indeed, it has been noted that the sharp differences in the tissue patterns that arise across distances of less than a micrometer during organogenesis, tissue remodeling, and tissue repair cannot be attributed solely to gradients of soluble growth factors. Instead, it has been proposed that it is the differential regulation of proliferation by localized differences in mechanical tension that in large part sculpts the micromorphology of developing, remodeling, and repairing tissues (21). Although many of the "upstream" components of the signal transduction pathways that serve to mediate the mechanoregulation of proliferation, such as integrins, focal adhesion kinase, and the small GTPases RhoA and Rac, have been characterized (2), there is little known about those components that serve to couple mechanical signaling directly to the central cell cycle regulatory machinery.

To begin to identify such "downstream" components of the signal transduction pathways that mediate the mechanoregulation of proliferation, we used two complementary systems: (i) a tissue culture system in which the level of mechanical tension developed by contractile cells in a three-dimensional collagen matrix is varied by altering the compliance of the matrix and (ii) a live rodent system in which the level of mechanical tension within an intact smooth muscle layer is varied by altering the resistance to the contraction of the smooth muscle.

Using these systems, we found that the cellular concentration of the F-box protein Skp2 is upregulated by increased mechanical tension. Skp2 is the substrate recognition subunit and limiting component of a SKP1–CUL1–F-box ubiquitin ligase complex that promotes proliferation primarily by targeting the cyclin-dependent kinase inhibitor $p27^{KIP1}$ for ubiquitination and, consequently, proteasomal degradation (7, 40, 44). Notably, whereas growth factors regulate Skp2 at the level of protein stability (8), we found that increased mechanical tension upregulates Skp2 expression at the level of transcription. Therefore, Skp2 expression is a point of convergence for signals from mechanical tension and growth factors in the regulation of proliferation.

* Corresponding author. Mailing address: Department of Internal Medicine, St. Louis VA Medical Center, John Cochran Division, 915 North Grand Blvd., St. Louis, MO 63106. Phone: (314) 652-4100, ext. 55298. Fax: (314) 362-5932. E-mail: sjweintraub@gmail.com.

† Present address: Department of Urology, University of Washington, Box 358050, 815 Mercer Street, Seattle, WA 98109.

‡ Present address: MIT Department of Biological Engineering, 500 Technology Square, NE47-380, Cambridge, MA 02139.

▽ Published ahead of print on 13 July 2009.

We next found that a consensus NFAT-binding site mediates the effects of mechanical tension on the activity of the Skp2 promoter. NFAT is a family of transcription factors that has four members that are activated by increased cytosolic calcium, designated NFATc1 (also known as NFATc or NFAT2), NFATc2 (also known as NFATp or NFAT1), NFATc3 (also known as NFAT4 or NFATx), and NFATc4 (also known as NFAT3) (12, 20). The calcium activates the phosphatase calcineurin through a calmodulin-dependent mechanism (3, 20). By dephosphorylating several serines in NFAT, calcineurin induces a conformational change in NFAT that exposes its nuclear localization signal and conceals its nuclear export signal, which results in its nuclear import (activation) (3, 20).

We found that NFATc1 is activated by increased mechanical tension and that the activation of NFATc1 is necessary for upregulation of Skp2 transcription that occurs in response to increased mechanical tension. Therefore, NFATc1 has a critical role in the mechanoregulation of proliferation. This is a notable finding because, whereas it is well established that cytosolic calcium increases when cells develop mechanical tension and that the increase in calcium promotes proliferation, the pathway(s) that mediates the effect of calcium on proliferation had not been defined. Therefore, we identified the first direct link between calcium signaling and the regulation of the central cell cycle machinery.

MATERIALS AND METHODS

Cell culture and transfections. Bladder smooth muscle cells (SMC; Cambrex) were cultured in SmGM2-medium (Cambrex), aortic SMC (Cell Applications, San Diego, CA) were cultured in SMC growth medium (Cell Applications), and foreskin fibroblasts were cultured in Dulbecco modified Eagle medium with 10% fetal bovine serum (FBS). To construct Skp2-luc, a 423-bp fragment corresponding to sequence from the 5′ flanking region of the human Skp2 gene (GenBank accession no. NT006576) was inserted between the MluI and BglII sites in the pGL3 promoter (Promega). SMC (~80% confluence on 100-mm tissue culture plates) were transfected with 4 μg of the indicated constructs by using Fugene6 (Roche) according to the manufacturer's protocol.

Collagen matrix assays. Cells were suspended in 1.4 mg of collagen (Vitrogen; Cohesion Technologies)/ml, and then the collagen was polymerized according to the manufacturer's protocol. Once the cells developed a spindlelike morphology (~6 h), the collagen matrices were either released from or left fixed to the tissue culture plate, and the cells were used in the assays described below.

Actin staining. SMC were cultured in collagen matrices for 24 h, rinsed with phosphate-buffered saline (PBS), fixed in 4% paraformaldehyde for 10 min, permeabilized with 0.1% Triton X-100 for 5 min, rinsed with PBS, and incubated with Alexa Fluor 488-phalloidin (Molecular Probes) for 20 min. After a rinse with PBS, the cells were visualized by fluorescence microscopy.

BrdU staining. SMC that were cultured in collagen matrices for 24 h were incubated in medium containing 30 μM bromodeoxyuridine (BrdU; Sigma) for an additional 4 h. Cells were isolated from the collagen matrices by incubation in 5 mg of type XI collagenase (Sigma)/ml and analyzed for BrdU uptake by immunofluorescence.

Bladder outlet obstruction. To create a complete bladder outlet obstruction, the urethras of 8- to 10-week-old anesthetized mice were ligated by using a 4-0 silk suture. Partial bladder outlet obstruction was created by placing a 22-gauge catheter alongside the urethra, tying a 4-0 silk ligature firmly around the urethra and the catheter, and then removing the catheter. At the indicated time points, bladders were excised and snap-frozen in liquid nitrogen or fixed in formalin and stained with hematoxylin and eosin.

Immunoblotting. SMC were isolated from the collagen matrices by incubation in 5 mg of type XI collagenase (Sigma)/ml and lysed in Triton buffer (0.5% Triton, 10 mM Tris [pH 8.6], 140 mM NaCl, 1.5 mM $MgCl_2$). Cells cultured on tissue culture plates were pelleted and lysed in sodium dodecyl sulfate (SDS) lysis buffer. Murine bladder smooth muscle tissue was snap-frozen, ground to powder, and lysed in SDS lysis buffer. To obtain nuclear lysate from murine bladder smooth muscle tissue, the tissue was excised and chopped into small pieces and then Dounce homogenized in ice-cold homogenization buffer (50 mM Tris-HCl [pH 7.5], 1.5 mM $MgCl_2$, 2 mM β-mercaptoethanol, 200 mM sucrose, 0.1% Triton X-100). To obtain nuclear lysate from cultured SMC, cells were scraped and incubated in homogenization buffer. The nuclei were pelleted, washed in homogenization buffer without Triton, and repelleted. The isolated nuclei were then lysed in SDS lysis buffer. Complete protease inhibitor cocktail (1×; Roche) and phosphatase inhibitor cocktails (Sigma) were present during the complete procedure. For dephosphorylation of NFATc1, human SMC were harvested in 1× passive lysis buffer (Promega) lacking phosphatase inhibitors, and then the lysate was incubated in 1× phosphatase buffer (Invitrogen) in either the presence or the absence of 1 U of calf intestinal alkaline phosphatase (Invitrogen)/μg at 37°C for 1 h. The following antibodies were used: Skp2 (catalog no. 51-1900) and Skp2 (catalog no. 32-3300) from Zymed; $p27^{KIP1}$ (c-19), $p21^{CIP1}$ (c-19), PCNA (PC10), β-tubulin (H-235), lamin A/C (N-18), and NFATc3 (F-1) from Santa Cruz; NFATc1 (7A6) from BD Pharmingen; and Erk (catalog no. 9102) and phospho-Erk (catalog no. 9106) from Cell Signaling.

RT-PCR. RNA was isolated from the cells in the collagen matrices by using TRIzol (Invitrogen) or from cells growing on tissue culture plates and mouse bladder smooth muscle layer using RNeasy (Qiagen). Reverse transcription-PCR (RT-PCR) was performed using RETROscript (Ambion) and PuReTaq Ready-To-Go PCR beads (GE Healthcare) with the following primers: Skp2 sense, 5′-ATGGGATTCCAGCAAGACTTCTGAA-3′; Skp2 antisense, 5′-GCTCAG GGAGGCACAGACAGGA-3′; $p27^{KIP1}$ sense, 5′-AGCCTGGAGCGGATGG AC-3′; $p27^{KIP1}$ antisense, 5′-CTTGGGCGTCTGCTCCACA-3′; b-myb sense, 5′-GATGTGCCGGAGCAGAGGGATAG-3′; b-myb antisense, 5′-GTCCATG GCCCCTTGACAAGGTC-3′; β-actin sense, 5′-GTGATGGTGGGCATGGGT CA-3′; β-actin antisense, 5′-TTAATGTCACGCACGATTTCCC-3′; GAPDH sense, 5′-GGTGAAGGTCGGAGTCAACG-3′; and GAPDH antisense, 5′-CA AAGTTGTCATGGATGACC-3′.

Luciferase assays. Luciferase assays were performed by using a luciferase assay system (Promega). Immunoblots for β-tubulin were performed to confirm that equal numbers of cells were assayed (data not shown).

Actinomycin D treatment. Human SMC were seeded in collagen matrices as described above. Approximately 6 h after the collagen had polymerized, the media was changed to SmGM-2 containing 1 μg of actinomycin D (Sigma)/ml, and the collagen matrices were either released from or left fixed to the tissue culture plate. At the indicated time points, RNA was isolated for RT-PCR analysis.

siRNA transfection. Small interfering RNAs (siRNAs) were transfected by using GeneEraser reagent (Stratagene) according to the manufacturer's protocol. The following siRNA sequences were used: scrambled sense, 5′-AUGUAU UGGCCUGUAUUAGUU-3′; scrambled antisense, 5′-CUAAUACAGGCCA AUACAUUU-3′; Skp2(A) sense, 5′-AAGGGAGUGACAAAGACUUUG-3′; Skp2(A) antisense, 5′-CAAAGUCUUUGUCACUCCCUU-3′; Skp2(B) sense, 5′-AAUCUAAGCCUGGAAGGCCUG-3′; Skp2(B) antisense, 5′-CAGGCCU UCCAGGCUUAGAUU-3′; NFATc1(A) sense, 5′-CGUAUGAGCUUCGGA UUGAUU-3′; NFATc1(A) antisense, 5′-UCAAUCCGAAGCUCAUACGUU-3′; NFATc1(B) sense, 5′-GAAACUCCGACAUUGAACUTT-3′; and NFATc1(B) antisense, 5′-TTAGUUCAAUGUCGGAGUUUC-3′. Cells were transfected twice at an interval of 24 h with Skp2 siRNAs and at an interval of 36 h with NFATc1 siRNAs.

ChIP assay. Mouse bladder smooth muscle tissue was chopped into small pieces, cross-linked with 1% formaldehyde in 1× PBS, and sonicated. Samples were processed according to the chromatin immunoprecipitation (ChIP) kit manufacturer's protocols (Upstate). DNA was recovered by using the phenol-chloroform method. The immunoprecipitated DNA was subjected to PCR assays with the following primer pairs: Skp2 promoter sense, 5′-CGTCTGGAAGGG ACTCAGAAG-3′; Skp2 promoter antisense, 5′-AACCCTCCAGATACCCAC AA-3′; β-globin sense, 5′-CCTGCCCTCTCTATCCTGTG-3′; and β-globin sense, 5′-GCAAATGTGTTGCCAAAAAG-3′. The NFATc1 antibody (H-110) was from Santa Cruz.

RESULTS

The development of mechanical tension is critical for smooth muscle proliferation. We initiated our studies by using a tissue culture system in which the effects of mechanical tension on cells such as SMC and fibroblasts can be assessed (4, 16, 17). Importantly, SMC and fibroblasts attempt to contract as they spread. If they are plated on a rigid substrate, such as a tissue culture dish, they develop mechanical tension as they

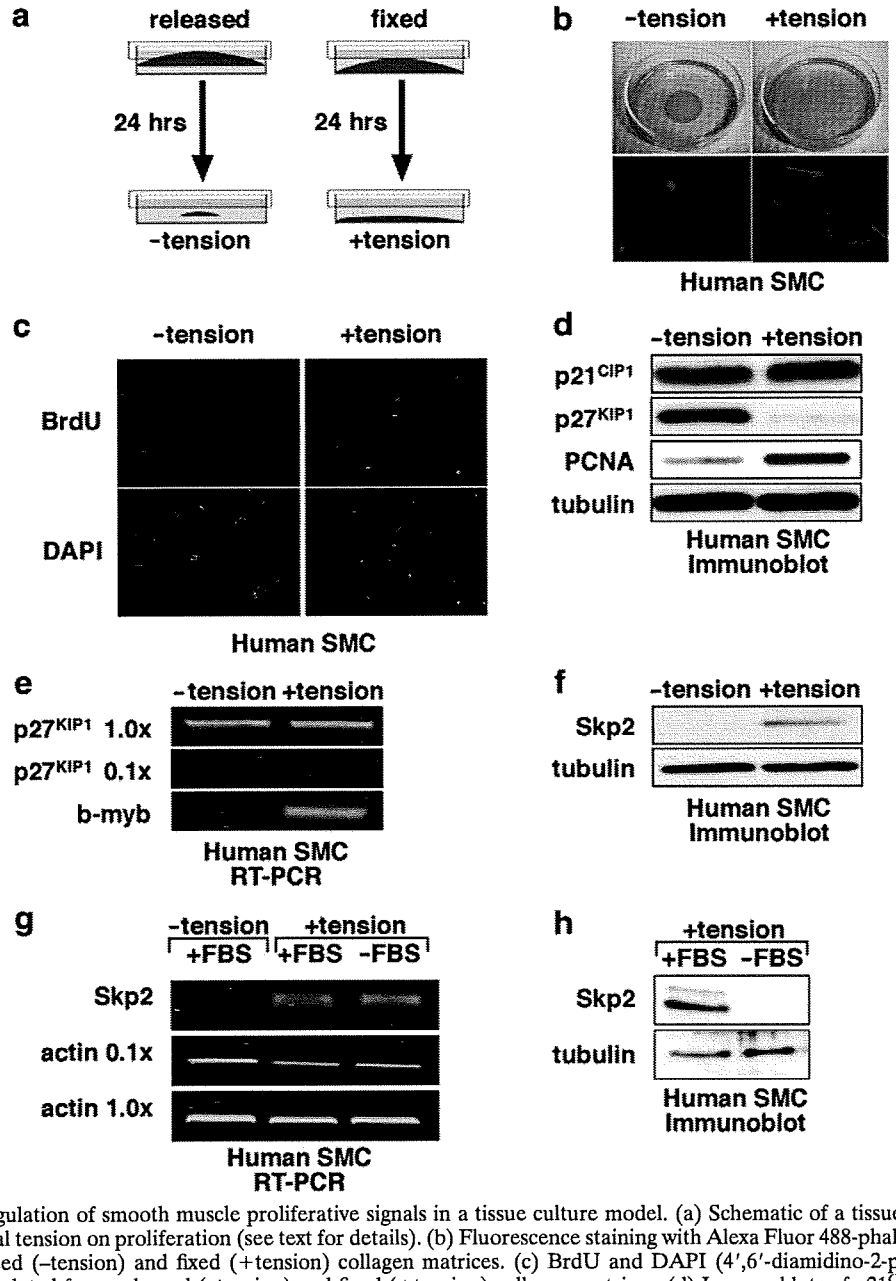

FIG. 1. Mechanoregulation of smooth muscle proliferative signals in a tissue culture model. (a) Schematic of a tissue culture system to study the effects of mechanical tension on proliferation (see text for details). (b) Fluorescence staining with Alexa Fluor 488-phalloidin for actin in human bladder SMC in released (–tension) and fixed (+tension) collagen matrices. (c) BrdU and DAPI (4′,6′-diamidino-2-phenylindole) staining of human bladder SMC isolated from released (–tension) and fixed (+tension) collagen matrices. (d) Immunoblots of $p21^{CIP1}$, $p27^{KIP1}$, PCNA, and β-tubulin in human bladder SMC isolated from released (–tension) and fixed (+tension) collagen matrices. (e) RT-PCR for $p27^{KIP1}$ and b-myb mRNA in human bladder SMC isolated from released (–tension) and fixed (+tension) collagen matrices (two different concentrations of the RT reaction products were loaded to confirm that the $p27^{KIP1}$ PCR was in the linear range). The level of b-myb mRNA was used as a proliferative marker. (f) Immunoblots of Skp2 and β-tubulin in human bladder SMC isolated from released (–tension) and fixed (+tension) collagen matrices. (g) RT-PCR for Skp2 and actin mRNA in human bladder SMC isolated from collagen matrices that were either released from (–tension) or left fixed to (+tension) the tissue culture dish in either serum-containing (+FBS) or serum-free (–FBS) media (two different concentrations of the RT reaction products were loaded to confirm that the actin PCR was in the linear range). (h) Immunoblots of Skp2 and β-tubulin in human bladder SMC isolated from collagen matrices that were left fixed to (+tension) the tissue culture dish in either serum-containing (+FBS) or serum-free (–FBS) medium.

attempt to contract against the resistance of the substrate (6, 13). The development of mechanical tension by the cells is necessary for proliferation to occur (6, 13). In the tissue culture model we used, cells are seeded in three-dimensional collagen matrices, and then each matrix is either released from the tissue culture dish and allowed to float freely in the medium or left fixed to the dish (Fig. 1a). The released matrices offer little resistance to the contraction of the cells; hence, only a relatively low level of mechanical tension develops within the cells. In contrast, the fixed matrices resist contraction, which allows for the development of an elevated level of mechanical tension within the cells (16). The difference in mechanical tension

within the released and fixed matrices is demonstrated by the finding that whereas stress fibers fail to develop in SMC in the released matrices, they form in cells in the fixed matrices (Fig. 1b). Thus, the released and fixed collagen matrices simulate the mechanical environments of nonstressed tissue and tissue in which the mechanical tension is increased, respectively. Importantly, whereas SMC in the released matrices do not proliferate, those in the fixed matrices do (few if any of the cells in a released matrix take up BrdU, while ca. 40% of the cells in a fixed matrix take up BrdU under the conditions of our assay) (Fig. 1c), indicating that the proliferation of the cells is regulated by mechanical tension in this system.

Skp2 is a node at which proliferative signals from soluble growth factors and mechanical tension are integrated in the regulation of proliferation in isolated SMC. To begin to understand the mechanism by which proliferative signals regulated by mechanical tension are coupled to the central cell cycle machinery, we first examined the effect of increased mechanical tension in SMC on the expression of two cyclin-dependent kinase inhibitors that have been implicated in the regulation of smooth muscle proliferation (42). We found that whereas the level of $p21^{CIP1}$ in the cells is unaffected by increased mechanical tension, the level of $p27^{KIP1}$ falls dramatically when mechanical tension is increased (Fig. 1d). The decrease in $p27^{KIP1}$ correlates with an increase in PCNA expression (Fig. 1d). Because $p27^{KIP1}$ serves to inhibit cell cycle progression (34), these findings suggested that $p27^{KIP1}$ has a role in the mechanoregulation of proliferation.

We therefore began to examine the mechanism by which smooth muscle $p27^{KIP1}$ is downregulated by increased mechanical tension. We found that changes in mechanical tension have no effect on the level of $p27^{KIP1}$ mRNA (Fig. 1e). It had previously been found that growth factors have no effect on $p27^{KIP1}$ mRNA levels; instead, growth factors downregulate $p27^{KIP1}$ by inducing its degradation (31). Therefore, we hypothesized that increased mechanical tension also downregulates $p27^{KIP1}$ by inducing its degradation.

The degradation of $p27^{KIP1}$ that occurs upon growth factor stimulation is mediated by the upregulation of expression of Skp2, a component of a ubiquitin ligase complex that targets $p27^{KIP1}$ for ubiquitination, and, consequently, proteasome-mediated degradation (7, 29, 40). Therefore, we examined the effect of increased mechanical tension on Skp2. We found that increased mechanical tension induces an increase in Skp2 (Fig. 1f), which suggested that the proliferative response that occurs in response to increased mechanical tension is mediated in part by Skp2.

To examine the mechanism by which an increase in mechanical tension increases the level of Skp2, we assessed the effect of mechanical tension on Skp2 mRNA. Growth factors increase Skp2 levels by stabilizing Skp2 protein (8, 48); in contrast, we found that the development of mechanical tension induces an increase in Skp2 mRNA (Fig. 1g). The increase of Skp2 mRNA in response to increased mechanical tension is growth factor independent, as indicated by the finding that the level of Skp2 mRNA is unaffected by serum deprivation (Fig. 1g). Serum deprivation, however, downregulates SMC Skp2 protein levels (Fig. 1 h). Therefore, whereas growth factors regulate Skp2 at the protein level, mechanical tension regulates Skp2 at the mRNA level. Hence, Skp2 expression is a point of convergence at which signaling from growth factors and mechanical tension are integrated.

Skp2 is a node at which proliferative signals from soluble growth factors and mechanical tension are integrated in the regulation of proliferation in intact smooth muscle tissue. We next wanted to confirm that these findings are relevant to the mechanoregulation of proliferation in intact smooth muscle tissue. The rodent urinary bladder is an ideal system for studies of the smooth muscle response to changes in mechanical tension for several reasons. (i) The mechanical tension in the bladder smooth muscle layer can readily be increased by obstructing the bladder outlet—the increase is due to smooth muscle contraction against the increased resistance to urine flow caused by the obstruction. (ii) The SMC in the rodent bladder proliferate in response to the increase in mechanical tension that develops when there is a bladder outlet obstruction (18, 24, 37, 45). (iii) The smooth muscle layer of the bladder is one of the thickest smooth muscle layers in the body. Therefore, it can serve as a source of a relatively large amount of smooth muscle tissue for detailed study (immunoblotting, RNA studies, etc.). (iv) The mechanical environment within the wall of an obstructed bladder can be simulated in tissue culture by allowing bladder SMC to contract against a semirigid support—as in the tissue culture system described above. This allows for the study of mechanical tension as an independent factor and it facilitates further analyses of findings that arise from studies performed on the intact bladder smooth muscle layer.

Strikingly, when we examined the effects of bladder outlet obstruction on the smooth muscle layer, our findings were precisely the same as the findings derived from isolated cells in the model described above. The increased tension in the bladder wall that develops when there is an obstruction has no effect on the level of $p21^{CIP1}$ in the smooth muscle, but it induces a decrease in the level of $p27^{KIP1}$ that correlates with an increase in PCNA (Fig. 2a). In addition, despite the fall in the level of $p27^{KIP1}$ protein, the level of the $p27^{KIP1}$ mRNA remains unchanged when there is an obstruction (Fig. 2b). Furthermore, the concentration of Skp2 protein is upregulated when there is an obstruction (Fig. 2c). Finally, the upregulation of Skp2 is mediated at least in part by an upregulation of Skp2 mRNA (Fig. 2d). These findings serve to validate our tissue culture system as an appropriate model for the study of the effects of mechanical tension on proliferation in intact smooth muscle tissue and, more importantly, when considered along with the findings from the tissue culture system, they strongly suggest that Skp2 is regulated at the mRNA level by changes in mechanical tension in intact smooth muscle.

We next wanted to confirm that Skp2 is truly important in the proliferative response to increased mechanical tension. We first used two different siRNAs to inhibit Skp2 expression in human bladder SMC. Inhibition of Skp2 expression increased the level of $p27^{KIP1}$ protein (Fig. 3a) and decreased proliferation (Fig. 3b). We then compared the effect of a partial bladder outlet obstruction in wild-type and $skp2^{-/-}$ mice (28) after 14 days. As expected based on previous studies of bladder outlet obstruction (18, 24, 37, 45), we found an extensive hyperplastic response in the bladder smooth muscle layer of the wild-type ($skp2^{+/+}$) mice (Fig. 3c). In contrast, however, we found that even though there is gross hypertrophy of the bladder smooth

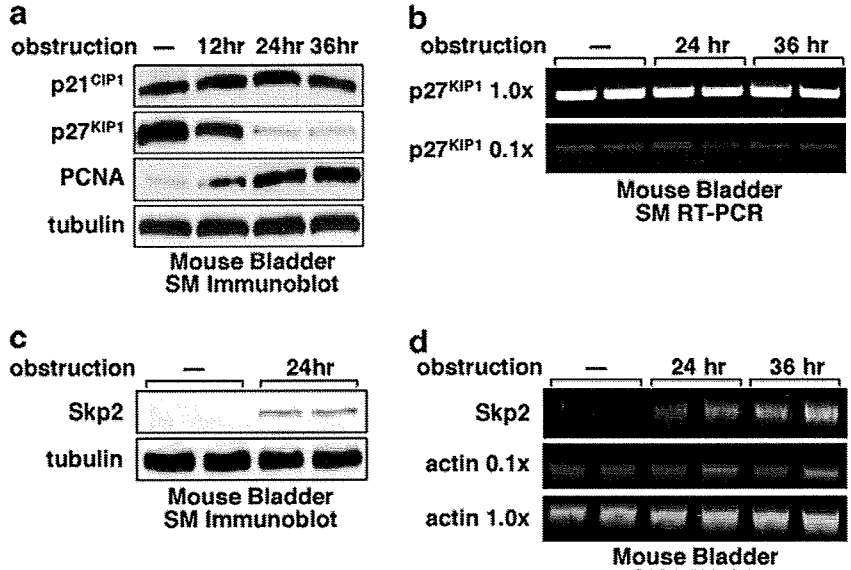

FIG. 2. Mechanoregulation of smooth muscle proliferative signals in intact tissue. (a) Immunoblots of $p21^{CIP1}$, $p27^{KIP1}$, PCNA, and β-tubulin in the smooth muscle layer of mouse bladders that were either unobstructed or completely obstructed for the time indicated (each lane in this and subsequent bladder obstruction experiments represents an assessment of the protein or RNA from an individual mouse). (b) RT-PCR for $p27^{KIP1}$ mRNA in the smooth muscle layer of mouse bladders that were either unobstructed or completely obstructed for the time indicated (two different concentrations of the RT reaction products were loaded to confirm that the $p27^{KIP1}$ PCR was in the linear range). (c) Immunoblots of Skp2 and β-tubulin in the smooth muscle layer of mouse bladders that were either unobstructed or completely obstructed for the time indicated. (d) RT-PCR for Skp2 and actin mRNA in the smooth muscle layer of mouse bladders that were either unobstructed or completely obstructed for the time indicated (two different concentrations of the RT reaction products were loaded to confirm that the actin PCR was in the linear range).

muscle layer in response to a bladder outlet obstruction in $skp2^{-/-}$ mice (Fig. 3c), the hyperplastic response is markedly decreased in the $skp2^{-/-}$ mice, as indicated by the relative paucity of nuclei in the bladder smooth muscle of $skp2^{-/-}$ mice (Fig. 3c). The decreased bladder smooth muscle hyperplastic response seems to be compensated for by increased cellular hypertrophy, as evidenced by the visibly increased thickness of the smooth muscle bundles in the obstructed bladders of $skp2^{-/-}$ mice (Fig. 3c). These were not surprising findings because they are consistent with the finding that hepatocytes increase in size but not number during liver regeneration after partial hepatectomy in $skp2^{-/-}$ mice (27) (which is in contrast to wild-type mice in which liver regeneration is primarily a proliferative response). In addition, in a manner analogous to the hypertrophy of the bladder wall that occurs in response to obstruction in the $skp2^{-/-}$ mice, the volume and mass of the livers of $skp2^{-/-}$ mice are completely restored after partial hepatectomy despite the lack of a hepatocyte proliferative response (27). Also consistent with our findings is the finding that there is a marked increase in the number of proliferating renal tubular cells in a murine model of unilateral ureteral obstruction in wild-type mice, but there is no change in the number of proliferating renal tubular cells in response to a ureteral obstruction in $skp2^{-/-}$ mice (41). Our results identify Skp2 as a critical mediator of the proliferative response that occurs in the bladder smooth muscle layer when there is bladder outlet obstruction—they therefore demonstrate the importance of mechanoregulation of Skp2 mRNA levels in the SMC hyperplastic response to increased tissue tension.

Mechanical tension regulates Skp2 mRNA levels in several types of cells. We next wanted to determine whether the regulation of Skp2 mRNA by mechanical tension is a generalized phenomenon that occurs in other tissues. Smooth muscle proliferation during vascular development and remodeling is regulated in part by localized mechanical forces within the vascular wall (21). Similarly, mechanical tension is thought to be important in the regulation of fibroblast proliferation during both tissue repair and pathological fibroproliferative responses (16, 21). Therefore, it is notable that, using the collagen matrix system described above, we found that Skp2 mRNA is upregulated by mechanical tension in primary human vascular SMC, primary human dermal fibroblasts (Fig. 4), and primary human lung fibroblasts (data not shown). The finding that Skp2 mRNA is regulated by mechanical tension in SMC and fibroblasts suggests that the regulation of Skp2 mRNA by changes in mechanical tension is a component of many, if not all, physiologic and pathological processes in which mechanical tension regulates proliferation.

A consensus binding site for the transcription factor NFAT has a critical role in the mechanoregulation Skp2 promoter activity. We next sought to determine the mechanism by which mechanical tension regulates Skp2 mRNA levels. Two independent findings initially suggested that mechanical tension regulates Skp2 at the transcriptional level: we found that (i) the stability of Skp2 mRNA is unaltered by changes in mechanical tension (Fig. 5a) and (ii) the activity of a reporter construct driven by a 423-bp sequence from the 5′-flanking region of the Skp2 gene (Skp2-luc) is increased in SMC in a fixed collagen matrix compared to its activity in a released matrix (Fig. 5b).

We next found that a consensus binding site for the calcium-regulated transcription factor NFAT has a role in mediating the effects of mechanical tension on the activity of the Skp2

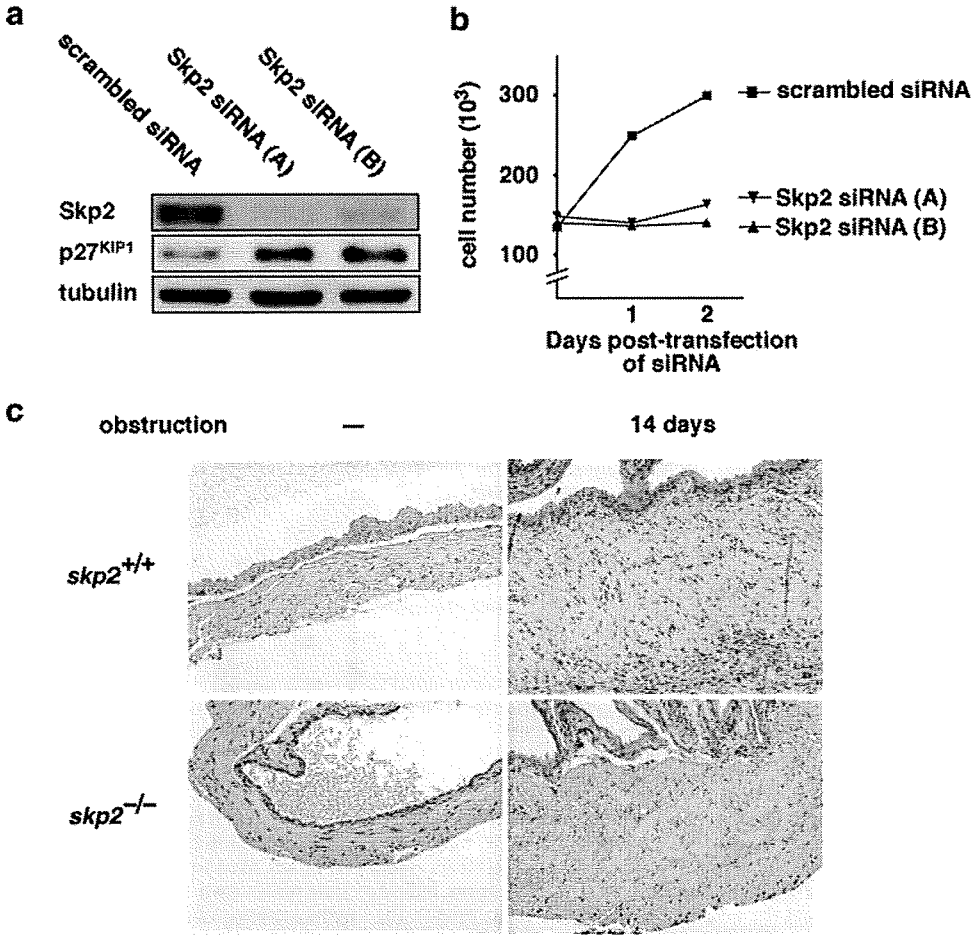

FIG. 3. Skp2 is required for bladder smooth muscle proliferation both in tissue culture and in intact tissue. (a) Immunoblots for Skp2, $p27^{KIP1}$, and tubulin in human bladder SMC that were adherent to a tissue culture dish and transfected with scrambled or two different Skp2-specific siRNAs. (b) Cell numbers at indicated time points of human SMC that were adherent to a tissue culture dish and transfected as in panel a. (c) The bladder walls of $skp2^{+/+}$ and $skp2^{-/-}$ mice that were either unobstructed or partially obstructed for 14 days and then fixed and stained with hematoxylin and eosin.

promoter: (i) its deletion abolishes the tension responsiveness of the Skp2 promoter in SMC (Fig. 5b) and (ii) its addition to a nonresponsive minimal promoter imparts tension responsiveness to the promoter in SMC (Fig. 5c). We therefore sought to determine whether NFAT activity increases in response to increased mechanical tension in an intact smooth muscle layer.

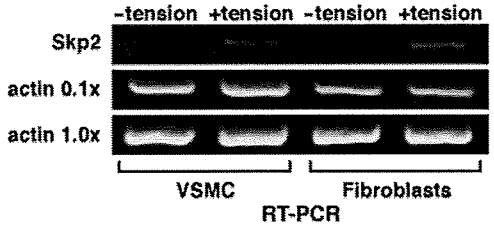

FIG. 4. Skp2 mRNA expression is regulated by mechanical tension in human vascular SMC and human fibroblasts. RT-PCR for Skp2 and actin mRNA in human vascular SMC and in human foreskin fibroblasts isolated from released (−tension) and fixed (+tension) collagen matrices (two different concentrations of the RT reaction products were loaded to confirm that the actin PCR was in the linear range).

To examine this, we assessed the effect of a bladder outlet obstruction on NFAT activity in the bladder smooth muscle layer of mice that are transgenic for an NFAT-responsive luciferase reporter construct (kindly provided by Benjamin Wilkins and Jeffery Molkentin) (46). This reporter is driven by NFAT-binding sites such that luciferase is expressed when an NFAT family member is activated in the tissue under study. We found that luciferase activity in the bladder smooth muscle layer increased three- to fourfold in response to bladder outlet obstruction in these mice (Fig. 5d). In addition, it had previously been demonstrated that an NFAT-dependent target, cyclooxygenase-2, is upregulated at the mRNA level by increased mechanical tension in isolated bladder SMC and in response to a bladder outlet obstruction in the bladder smooth muscle layer (22, 32). Together, these findings provided evidence that an NFAT family member(s) has a role in the upregulation of Skp2 transcription that occurs when mechanical tension is increased in smooth muscle tissue.

Notably, the NFAT site is conserved in the human and mouse Skp2 promoters (Fig. 6a) and its sequence is an exact match with the NFAT-binding site in the human interleukin-2

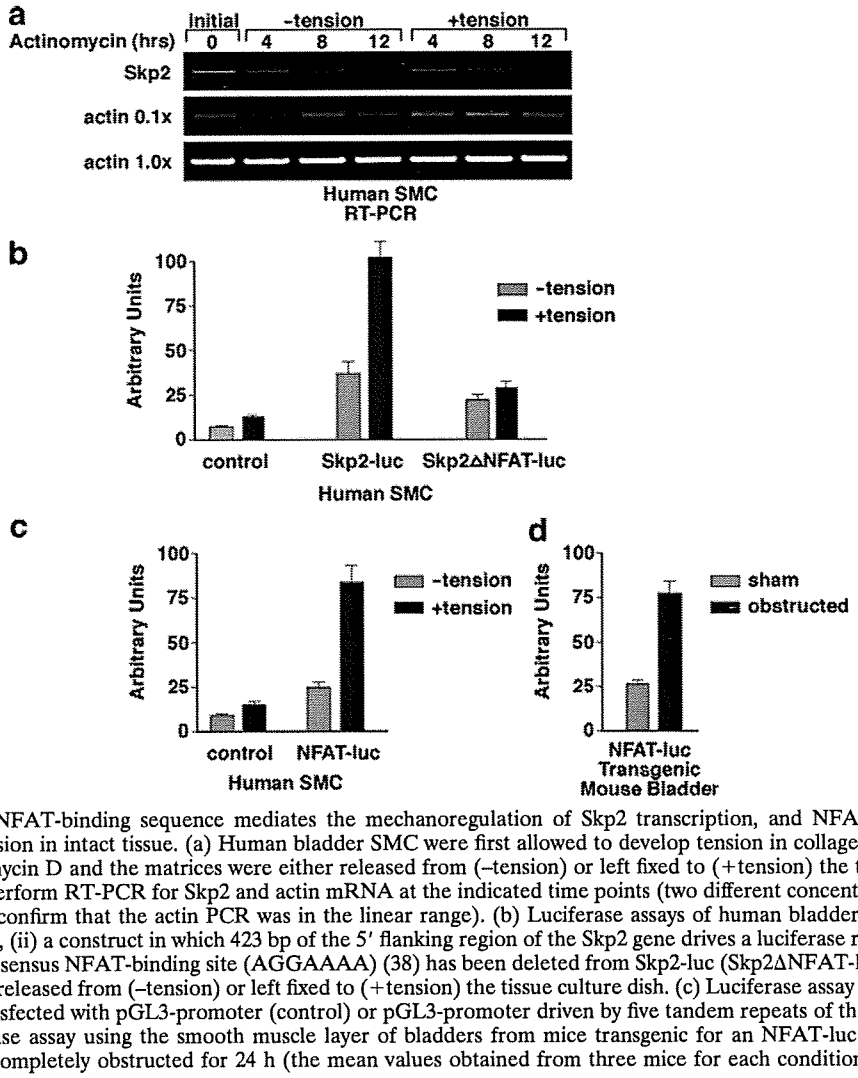

FIG. 5. A consensus NFAT-binding sequence mediates the mechanoregulation of Skp2 transcription, and NFAT activity is increased by increased mechanical tension in intact tissue. (a) Human bladder SMC were first allowed to develop tension in collagen matrices. The cells were then treated with actinomycin D and the matrices were either released from (–tension) or left fixed to (+tension) the tissue culture dish ("0 h"). Cells were harvested to perform RT-PCR for Skp2 and actin mRNA at the indicated time points (two different concentrations of the RT reaction products were loaded to confirm that the actin PCR was in the linear range). (b) Luciferase assays of human bladder SMC transfected with (i) pGL3-promoter (control), (ii) a construct in which 423 bp of the 5′ flanking region of the Skp2 gene drives a luciferase reporter (Skp2-luc), or (iii) a construct in which a consensus NFAT-binding site (AGGAAAA) (38) has been deleted from Skp2-luc (Skp2ΔNFAT-luc) isolated from collagen matrices that were either released from (–tension) or left fixed to (+tension) the tissue culture dish. (c) Luciferase assay as in panel B, except using human bladder SMC transfected with pGL3-promoter (control) or pGL3-promoter driven by five tandem repeats of the Skp2 NFAT-binding site (NFAT-luc). (d) Luciferase assay using the smooth muscle layer of bladders from mice transgenic for an NFAT-luc reporter that were either unobstructed (sham) or completely obstructed for 24 h (the mean values obtained from three mice for each condition).

(IL-2) promoter, the prototypical NFAT-regulated promoter (38) (Fig. 6a). Furthermore, there is extensive conservation between the surrounding sequence of the NFAT site in the human and mouse Skp2 promoters and the IL-2 NFAT site in that the region 5′ to each of the sites is GA rich and the sequence NCNG is conserved 3′ to the NFAT-binding site in all three promoters (Fig. 6a). These findings provide further evidence that a member(s) of the NFAT family of transcription factors mediates the mechanoregulation of Skp2 transcription.

NFATc1 undergoes dephosphorylation and nuclear translocation in response to increased mechanical tension. NFAT family members are activated when they are dephosphorylated by the phosphatase calcineurin. Upon activation, they are imported into the nucleus where they bind their cognate promoter-binding sites (20). There are four calcineurin-regulated NFAT isoforms, NFATc1 to NFATc4. Their expression varies between different types of smooth muscle (5, 15, 19, 25, 39, 49), and there are instances in which the individual NFAT isoforms are differentially regulated within the same type of SMC (5, 49). Once in the nucleus, the localization of NFAT proteins is regulated by a series of kinases; it is likely that these kinases mediate the differential regulation of the individual NFAT isoforms (19).

We examined the most well-studied smooth muscle NFAT proteins, NFATc1 and NFATc3, in human bladder SMC. It would be difficult to examine NFAT activation using the collagen matrix assay, because tension is relieved as the cells are isolated from the collagen matrix and NFAT proteins are rapidly exported from the nucleus after cessation of the activating signal (43). However, cells develop tension as they spread on the rigid surface of a tissue culture dish (6, 13). Therefore, we initially used adhesion and subsequent spreading as a surrogate for the development of tension in a collagen matrix. We found little or no change in nuclear NFATc3 upon adhesion (Fig. 6b). However, in the same lysates, we found that a rapidly migrating form of NFATc1 develops in the adherent, spread cells that is not present in suspended cells (Fig. 6b). Notably, a comparison of nuclear lysates and whole-cell lysates reveals that relative to the other forms of NFATc1, this form is concentrated in the nucleus (Fig. 6b), which is consistent with dephosphorylation mediating the nuclear localization of NFATc1. Indeed, phosphatase treatment of whole-cell lysates

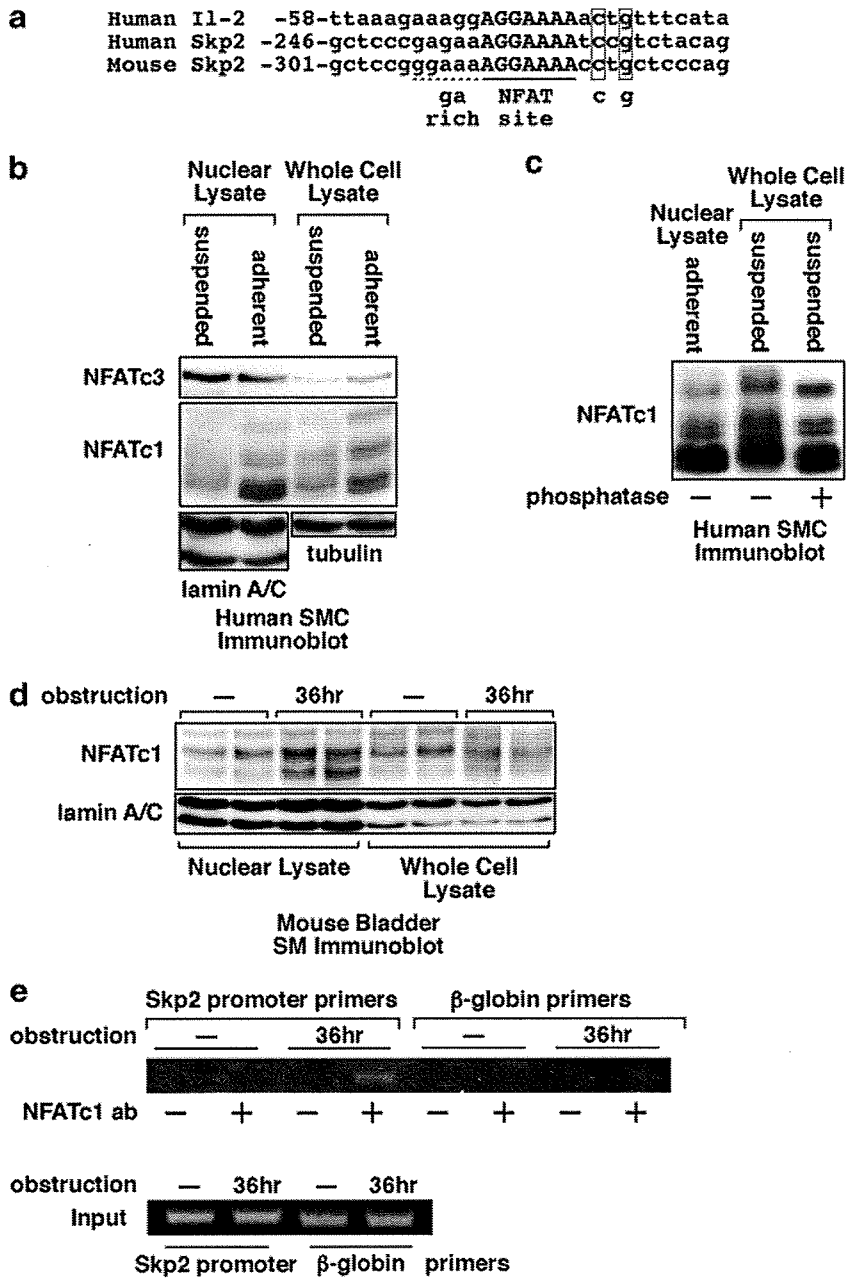

FIG. 6. NFATc1 directly targets the Skp2 promoter. (a) Comparison of the NFAT-binding site and surrounding sequence in the human and mouse Skp2 promoters with the NFAT-binding site and surrounding sequence in the human IL-2 promoter, the prototypical NFAT-binding site (38). (b) Immunoblot of NFATc3 and NFATc1 in nuclear lysates and whole-cell lysates of adherent and suspended human bladder SMC. Lamin A/C and tubulin were used as loading controls. (c) Immunoblot of NFATc1 in whole-cell lysates of suspended human bladder SMC treated with calf intestinal alkaline phosphatase as indicated. Nuclear lysates of adherent cells were used as a reference. (d) Immunoblot for NFATc1 in nuclear lysates and whole-cell lysates from the smooth muscle layer of mouse bladders that were partially obstructed as indicated. Lamin A/C was used as a loading control. (e) ChIP assay of the endogenous Skp2 promoter in the bladder smooth muscle layer of mouse bladders that were either unobstructed or partially obstructed as indicated. Primers targeted to the 5′-untranslated region of the β-globin gene were used as a control for specificity.

of suspended cells results in the formation of an NFATc1 protein that migrates in the same position as this rapidly migrating form (Fig. 6c). Similarly, the nuclear levels of the fastest-migrating form of NFATc1 increases in the bladder smooth muscle layer in response to a bladder outlet obstruction and this form is concentrated in the nucleus (Fig. 6d). Together, these data strongly suggest that increased mechanical tension induces the dephosphorylation and consequent nuclear localization of NFATc1.

NFATc1 is a critical mediator in the regulation of Skp2 transcription by changes in mechanical tension. We next found that NFATc1 binds to the Skp2 promoter in the bladder

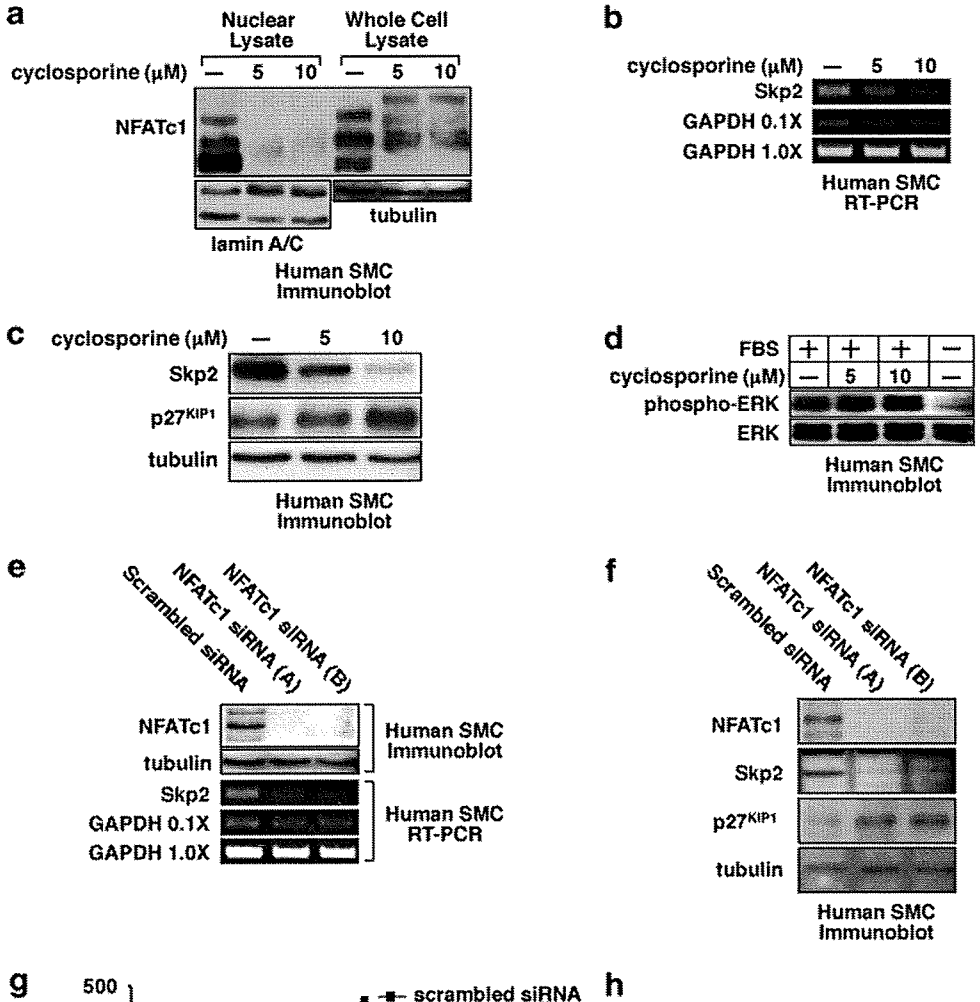

FIG. 7. NFATc1 regulates Skp2 expression. (a) Immunoblot for NFATc1 in human bladder SMC that were adherent to a tissue culture dish and treated with indicated concentrations of cyclosporine for 12 h. (b) RT-PCR for Skp2 and GAPDH mRNA in human bladder SMC that were adherent to a tissue culture dish and treated with cyclosporine as in panel a (two different concentrations of the RT reaction products were loaded to confirm that the GAPDH PCR was in the linear range). (c) Immunoblots for Skp2, $p27^{KIP1}$, and tubulin in human bladder SMC that were adherent to a tissue culture dish and treated with cyclosporine as in panel a. (d) Immunoblots for Erk and phospho-Erk in human bladder SMC that were adherent to a tissue culture dish and treated with cyclosporine as in panel a. Cells grown in the absence of serum (FBS) were used as a positive control for dephosphorylated Erk. (e) Immunoblots for NFATc1 and tubulin and RT-PCR for Skp2 and GAPDH mRNA in human bladder SMC that were adherent to a tissue culture dish and transfected with scrambled or two different NFATc1-specific siRNAs (two different concentrations of the RT reaction products were loaded to confirm that the GAPDH PCR was in the linear range). (f) Immunoblots for NFATc1, Skp2, $p27^{KIP1}$, and tubulin in human bladder SMC that were adherent to a tissue culture dish and then transfected as in panel e. (g) Cell numbers at indicated time points of human SMC that were adherent to a tissue culture dish and transfected as in panel e. (h) DAPI-stained nuclei of human bladder SMC 120 h after the cells were transfected as in panel e. Similar results were obtained with both NFATc1 siRNAs.

smooth muscle layer when there is a bladder outlet obstruction (Fig. 6e), which provided evidence for a role for NFATc1 in mediating the upregulation of Skp2 transcription in response to increased mechanical tension. To further examine whether NFATc1 does indeed have role in the mechanoregulation of Skp2 transcription, we treated bladder SMC with the calcineurin inhibitor cyclosporine and found that it blocks NFATc1 nuclear localization (Fig. 7a) and inhibits Skp2

mRNA expression (Fig. 7b) and Skp2 protein expression (Fig. 7c). Importantly, the effect of cyclosporine treatment on Skp2 mRNA is not due to a generalized effect on proliferative signals, since cyclosporine treatment does not inhibit ERK phosphorylation at concentrations that block NFATc1 activity (Fig. 7d). Strikingly, these findings are consistent with a recent report that systemically administered cyclosporine inhibits the bladder smooth muscle response to obstruction in a rabbit model of bladder outlet obstruction (10).

To confirm that NFATc1 has a role in the regulation of Skp2 expression in SMC, we used siRNA to inhibit NFATc1 expression. Inhibition of NFATc1 protein expression decreased Skp2 mRNA (Fig. 7e) and Skp2 protein (Fig. 7f) and increased $p27^{KIP1}$ protein (Fig. 7f), confirming a role for NFATc1 in the mechanoregulation of Skp2 transcription and proliferative signaling downstream of Skp2. Interestingly, although NFATc1 siRNA blocks cellular proliferation (Fig. 7g), a component of the block is due to cell death since we found that inhibition of NFATc1 expression ultimately caused nuclear condensation (Fig. 7 h), which is consistent with the previous findings that NFAT inhibition results in cardiomyocyte apoptosis (35) and that a constitutively active form of NFATc1 is antiapoptotic in fibroblasts (30). Therefore, NFATc1 activates both proliferative and survival signals in the mechanoregulation of proliferation.

DISCUSSION

We have demonstrated that signaling from mechanical tension upregulates Skp2 transcription. It has previously been shown that adhesion is necessary to support Skp2 transcription (8). We have added a critical refinement to this finding by demonstrating that adhesion per se, while necessary, is not sufficient for the upregulation of Skp2 transcription; we found that even when a cell is adherent to collagen, it must develop and maintain mechanical tension to support transcription of Skp2. Indeed, we found that the changes in NFATc1 that occur when isolated bladder SMC adhere to a tissue culture dish (Fig. 5b) are similar to the changes in NFATc1 that occur in the bladder smooth muscle layer in response to the increase in bladder wall tension that occurs when there is a bladder outlet obstruction (Fig. 5d) and that the changes are due to dephosphorylation (Fig. 5c), suggesting that the changes in NFATc1 that occur upon adhesion are due to the development of mechanical tension once the adherent cell spreads. Further supporting this argument is the finding that the level of Skp2 mRNA in adherent cells can be regulated by changes in cell shape (26). By examining NFATc1 activation and Skp2 mRNA expression in intact tissue, we have demonstrated the importance of the distinction between adhesion per se and the development of mechanical tension by an adherent cell.

Smooth muscle contraction is initiated by an increase in sarcoplasmic calcium. Calcium binds and thereby activates calmodulin, which in turn activates calmodulin-dependent myosin light-chain kinase. By catalyzing myosin phosphorylation, calmodulin-dependent myosin light-chain kinase activates actin-myosin cross-bridge cycling, causing mechanical force to be generated (1). Calcium/calmodulin signaling is also essential for cell cycle progression; however, the downstream effectors that mediate the calcium/calmodulin proliferative signals have not previously been identified (23). One proximal target of calcium/calmodulin signaling is the phosphatase calcineurin and it has been established that the activation of calcineurin is critical for the proliferative effects of increased calcium (23). This is notable because when calcineurin is activated, it dephosphorylates NFAT, and thereby induces its nuclear translocation. Therefore, our finding that NFATc1 mediates the mechanoregulation of Skp2 transcription identifies NFATc1 as a direct link between the proliferative signals mediated by the calcium/calmodulin/calcineurin pathway and the central cell cycle machinery. Our findings therefore in part explain the role of calcium in proliferation.

The E2F family of transcription factors has a central role in the regulation of proliferation (33). Hence, it is notable that E2F has a role in the transcriptional activation of Skp2 in mouse embryo fibroblasts (50) and in tumor cells that express high levels of E2F (51). However, it has been shown that E2F is not important for the transcriptional activation of Skp2 in tumor cells that only express low levels of E2F or in human foreskin fibroblasts (51). This is notable because we found that serum starvation has no effect on Skp2 mRNA levels in human bladder SMC (Fig. 1g) and the Pagano and Krek laboratories found that serum starvation has no effect on Skp2 mRNA levels in human diploid fibroblasts (8, 48). Because serum starvation induces the pocket proteins to bind to and inactivate E2F proteins (11), these findings imply that E2F does not have a significant role in the transcriptional activation of Skp2 in human SMC and human diploid fibroblasts and our finding specifically implies that E2F does not have a role in the mechanoregulation of Skp2 transcription in human bladder SMC. It is important to note, however, that E2F may have a role in the mechanoregulation of Skp2 transcription in other cell types.

Finally, our finding that Skp2 is regulated by mechanical tension at the mRNA level in vascular smooth muscle and fibroblasts, in addition to bladder smooth muscle, suggests that the regulation of Skp2 transcription by changes in mechanical tension is a component of many, if not all, physiologic and pathological processes in which mechanical tension regulates cellular proliferation. Intriguingly, calcineurin-mediated NFATc1 activation has a critical role in cardiac valve and outflow tract development (9, 14, 36), as well as osteoblast proliferation during skeletal development and repair (47). These are processes in which the mechanoregulation of proliferation is likely to have a critical role. It is possible that Skp2 is an NFATc1 target in each of these.

ACKNOWLEDGMENTS

We thank Neil Clipstone for helpful discussions, Benjamin Wilkins and Jeffery Molkentin for kindly providing the NFAT-luciferase transgenic mice, S. He and K. Grapperhaus for technical assistance, and the Morphology Core of the Washington University Digestive Diseases Research Core Center for preparation of the histology specimens.

This study was supported by grants from the National Institutes of Health (NIH) and the Midwest Stone Institute to S.J.W. and an NIH grant to P.F.A.

REFERENCES

1. **Allen, B. G., and M. P. Walsh.** 1994. The biochemical basis of the regulation of smooth-muscle contraction. Trends Biochem. Sci. **19**:362–368.
2. **Assoian, R. K., and M. A. Schwartz.** 2001. Coordinate signaling by integrins and receptor tyrosine kinases in the regulation of G_1 phase cell-cycle progression. Curr. Opin. Genet. Dev. **11**:48–53.

3. **Beals, C. R., N. A. Clipstone, S. N. Ho, and G. R. Crabtree.** 1997. Nuclear localization of NF-ATc by a calcineurin-dependent, cyclosporin-sensitive intramolecular interaction. Genes Dev. **11**:824–834.
4. **Bell, E., B. Ivarsson, and C. Merrill.** 1979. Production of a tissue-like structure by contraction of collagen lattices by human fibroblasts of different proliferative potential in vitro. Proc. Natl. Acad. Sci. USA **76**:1274–1278.
5. **Boss, V., K. L. Abbott, X. F. Wang, G. K. Pavlath, and T. J. Murphy.** 1998. The cyclosporin A-sensitive nuclear factor of activated T cells (NFAT) proteins are expressed in vascular smooth muscle cells. Differential localization of NFAT isoforms and induction of NFAT-mediated transcription by phospholipase C-coupled cell surface receptors. J. Biol. Chem. **273**:19664–19671.
6. **Burridge, K.** 1981. Are stress fibres contractile? Nature **294**:691–692.
7. **Carrano, A. C., E. Eytan, A. Hershko, and M. Pagano.** 1999. SKP2 is required for ubiquitin-mediated degradation of the CDK inhibitor p27. Nat. Cell Biol. **1**:193–199.
8. **Carrano, A. C., and M. Pagano.** 2001. Role of the F-box protein Skp2 in adhesion-dependent cell cycle progression. J. Cell Biol. **153**:1381–1390.
9. **Chang, C. P., J. R. Neilson, J. H. Bayle, J. E. Gestwicki, A. Kuo, K. Stankunas, I. A. Graef, and G. R. Crabtree.** 2004. A field of myocardial-endocardial NFAT signaling underlies heart valve morphogenesis. Cell **118**:649–663.
10. **Clement, M. R., D. P. Delaney, J. C. Austin, J. Sliwoski, G. C. Hii, D. A. Canning, M. E. DiSanto, S. K. Chacko, and S. A. Zderic.** 2006. Activation of the calcineurin pathway is associated with detrusor decompensation: a potential therapeutic target. J. Urol. **176**:1225–1229.
11. **Cobrinik, D.** 2005. Pocket proteins and cell cycle control. Oncogene **24**: 2796–2809.
12. **Crabtree, G. R., and E. N. Olson.** 2002. NFAT signaling: choreographing the social lives of cells. Cell **109**(Suppl.):S67–S79.
13. **Curtis, A. S., and G. M. Seehar.** 1978. The control of cell division by tension or diffusion. Nature **274**:52–53.
14. **de la Pompa, J. L., L. A. Timmerman, H. Takimoto, H. Yoshida, A. J. Elia, E. Samper, J. Potter, A. Wakeham, L. Marengere, B. L. Langille, G. R. Crabtree, and T. W. Mak.** 1998. Role of the NF-ATc transcription factor in morphogenesis of cardiac valves and septum. Nature **392**:182–186.
15. **Gonzalez Bosc, L. V., M. K. Wilkerson, K. N. Bradley, D. M. Eckman, D. C. Hill-Eubanks, and M. T. Nelson.** 2004. Intraluminal pressure is a stimulus for NFATc3 nuclear accumulation: role of calcium, endothelium-derived nitric oxide, and cGMP-dependent protein kinase. J. Biol. Chem. **279**:10702–10709.
16. **Grinnell, F.** 2000. Fibroblast-collagen-matrix contraction: growth-factor signalling and mechanical loading. Trends Cell Biol. **10**:362–365.
17. **Grinnell, F.** 1994. Fibroblasts, myofibroblasts, and wound contraction. J. Cell Biol. **124**:401–404.
18. **Hanai, T., F. H. Ma, S. Matsumoto, Y. C. Park, and T. Kurita.** 2002. Partial outlet obstruction of the rat bladder induces a stimulatory response on proliferation of the bladder smooth muscle cells. Int. Urol. Nephrol. **34**:37–42.
19. **Hill-Eubanks, D. C., M. F. Gomez, A. S. Stevenson, and M. T. Nelson.** 2003. NFAT regulation in smooth muscle. Trends Cardiovasc. Med. **13**:56–62.
20. **Hogan, P. G., L. Chen, J. Nardone, and A. Rao.** 2003. Transcriptional regulation by calcium, calcineurin, and NFAT. Genes Dev. **17**:2205–2232.
21. **Huang, S., and D. E. Ingber.** 1999. The structural and mechanical complexity of cell-growth control. Nat. Cell Biol. **1**:E131–E138.
22. **Iniguez, M. A., S. Martinez-Martinez, C. Punzon, J. M. Redondo, and M. Fresno.** 2000. An essential role of the nuclear factor of activated T cells in the regulation of the expression of the cyclooxygenase-2 gene in human T lymphocytes. J. Biol. Chem. **275**:23627–23635.
23. **Kahl, C. R., and A. R. Means.** 2003. Regulation of cell cycle progression by calcium/calmodulin-dependent pathways. Endocrinol. Rev. **24**:719–736.
24. **Lindner, P., A. Mattiasson, L. Persson, and B. Uvelius.** 1988. Reversibility of detrusor hypertrophy and hyperplasia after removal of infravesical outflow obstruction in the rat. J. Urol. **140**:642–646.
25. **Liu, Z., C. Zhang, N. Dronadula, Q. Li, and G. N. Rao.** 2005. Blockade of nuclear factor of activated T cells activation signaling suppresses balloon injury-induced neointima formation in a rat carotid artery model. J. Biol. Chem. **280**:14700–14708.
26. **Mammoto, A., S. Huang, K. Moore, P. Oh, and D. E. Ingber.** 2004. Role of RhoA, mDia, and ROCK in cell shape-dependent control of the Skp2-$p27^{Kip1}$ pathway and the G_1/S transition. J. Biol. Chem. **274**:28828–28835.
27. **Minamishima, Y. A., and K. Nakayama.** 2002. Recovery of liver mass without proliferation of hepatocytes after partial hepatectomy in Skp2-deficient mice. Cancer Res. **62**:995–999.
28. **Nakayama, K., H. Nagahama, Y. A. Minamishima, M. Matsumoto, I. Nakamichi, K. Kitagawa, M. Shirane, R. Tsunematsu, T. Tsukiyama, N. Ishida, M. Kitagawa, K. Nakayama, and S. Hatakeyama.** 2000. Targeted disruption of Skp2 results in accumulation of cyclin E and $p27^{Kip1}$, polyploidy, and centrosome overduplication. EMBO J. **19**:2069–2081.
29. **Nakayama, K. I., S. Hatakeyama, and K. Nakayama.** 2001. Regulation of the cell cycle at the G_1-S transition by proteolysis of cyclin E and $p27^{Kip1}$. Biochem. Biophys. Res. Commun. **282**:853–860.
30. **Neal, J. W., and N. A. Clipstone.** 2003. A constitutively active NFATc1 mutant induces a transformed phenotype in 3T3-L1 fibroblasts. J. Biol. Chem. **278**:17246–17254.
31. **Pagano, M., S. W. Tam, A. M. Theodoras, P. Beer-Romero, G. Del Sal, V. Chau, P. R. Yew, G. F. Draetta, and M. Rolfe.** 1995. Role of the ubiquitin-proteasome pathway in regulating abundance of the cyclin-dependent kinase inhibitor p27. Science **269**:682–685.
32. **Park, J. M., T. Yang, L. J. Arend, A. M. Smart, J. B. Schnermann, and J. P. Briggs.** 1997. Cyclooxygenase-2 is expressed in bladder during fetal development and stimulated by outlet obstruction. Am. J. Physiol. **273**:F538–F544.
33. **Polager, S., and D. Ginsberg.** 2008. E2F: at the crossroads of life and death. Trends Cell Biol. **18**:528–535.
34. **Polyak, K., J. Y. Kato, M. J. Solomon, C. J. Sherr, J. Massague, J. M. Roberts, and A. Koff.** 1994. $p27^{Kip1}$, a cyclin-Cdk inhibitor, links transforming growth factor-beta and contact inhibition to cell cycle arrest. Genes Dev. **8**:9–22.
35. **Pu, W. T., Q. Ma, and S. Izumo.** 2003. NFAT transcription factors are critical survival factors that inhibit cardiomyocyte apoptosis during phenylephrine stimulation in vitro. Circ. Res. **92**:725–731.
36. **Ranger, A. M., M. J. Grusby, M. R. Hodge, E. M. Gravallese, F. C. de la Brousse, T. Hoey, C. Mickanin, H. S. Baldwin, and L. H. Glimcher.** 1998. The transcription factor NF-ATc is essential for cardiac valve formation. Nature **392**:186–190.
37. **Saito, M., P. A. Longhurst, M. Murphy, F. C. Monson, A. J. Wein, and R. M. Levin.** 1994. 3H-thymidine uptake by the rat urinary bladder after partial outflow obstruction. Neurourol. Urodyn. **13**:63–69.
38. **Schubert, W., X. Y. Yang, T. T. Yang, S. M. Factor, M. P. Lisanti, J. D. Molkentin, M. Rincon, and C. W. Chow.** 2003. Requirement of transcription factor NFAT in developing atrial myocardium. J. Cell Biol. **161**:861–874.
39. **Stevenson, A. S., M. F. Gomez, D. C. Hill-Eubanks, and M. T. Nelson.** 2001. NFAT4 movement in native smooth muscle. A role for differential Ca^{2+} signaling. J. Biol. Chem. **276**:15018–15024.
40. **Sutterluty, H., E. Chatelain, A. Marti, C. Wirbelauer, M. Senften, U. Muller, and W. Krek.** 1999. p45SKP2 promotes $p27^{Kip1}$ degradation and induces S phase in quiescent cells. Nat. Cell Biol. **1**:207–214.
41. **Suzuki, S., H. Fukasawa, K. Kitagawa, C. Uchida, T. Hattori, T. Isobe, T. Oda, T. Misaki, N. Ohashi, K. Nakayama, K. I. Nakayama, A. Hishida, T. Yamamoto, and M. Kitagawa.** 2007. Renal damage in obstructive nephropathy is decreased in Skp2-deficient mice. Am. J. Pathol. **171**:473–483.
42. **Tanner, F. C., M. Boehm, L. M. Akyurek, H. San, Z. Y. Yang, J. Tashiro, G. J. Nabel, and E. G. Nabel.** 2000. Differential effects of the cyclin-dependent kinase inhibitors $p27^{Kip1}$, $p21^{Cip1}$, and $p16^{Ink4}$ on vascular smooth muscle cell proliferation. Circulation **101**:2022–2025.
43. **Timmerman, L. A., N. A. Clipstone, S. N. Ho, J. P. Northrop, and G. R. Crabtree.** 1996. Rapid shuttling of NF-AT in discrimination of Ca2+ signals and immunosuppression. Nature **383**:837–840.
44. **Tsvetkov, L. M., K. H. Yeh, S. J. Lee, H. Sun, and H. Zhang.** 1999. $p27^{Kip1}$ ubiquitination and degradation is regulated by the SCF(Skp2) complex through phosphorylated Thr187 in p27. Curr. Biol. **9**:661–664.
45. **Uvelius, B., L. Persson, and A. Mattiasson.** 1984. Smooth muscle cell hypertrophy and hyperplasia in the rat detrusor after short-time infravesical outflow obstruction. J. Urol. **131**:173–176.
46. **Wilkins, B. J., Y. S. Dai, O. F. Bueno, S. A. Parsons, J. Xu, D. M. Plank, F. Jones, T. R. Kimball, and J. D. Molkentin.** 2004. Calcineurin/NFAT coupling participates in pathological, but not physiological, cardiac hypertrophy. Circ. Res. **94**:110–118.
47. **Winslow, M. M., M. Pan, M. Starbuck, E. M. Gallo, L. Deng, G. Karsenty, and G. R. Crabtree.** 2006. Calcineurin/NFAT signaling in osteoblasts regulates bone mass. Dev. Cell **10**:771–782.
48. **Wirbelauer, C., H. Sutterluty, M. Blondel, M. Gstaiger, M. Peter, F. Reymond, and W. Krek.** 2000. The F-box protein Skp2 is a ubiquitylation target of a Cul1-based core ubiquitin ligase complex: evidence for a role of Cul1 in the suppression of Skp2 expression in quiescent fibroblasts. EMBO J. **19**: 5362–5375.
49. **Yellaturu, C. R., S. K. Ghosh, R. K. Rao, L. K. Jennings, A. Hassid, and G. N. Rao.** 2002. A potential role for nuclear factor of activated T cells in receptor tyrosine kinase and G-protein-coupled receptor agonist-induced cell proliferation. Biochem. J. **368**:183–190.
50. **Yung, Y., J. L. Walker, J. M. Roberts, and R. K. Assoian.** 2007. A Skp2 autoinduction loop and restriction point control. J. Cell Biol. **178**:741–747.
51. **Zhang, L., and C. Wang.** 2006. F-box protein Skp2: a novel transcriptional target of E2F. Oncogene **25**:2615–2627.

p53-Altered *FBXW7* Expression Determines Poor Prognosis in Gastric Cancer Cases

Takehiko Yokobori,[1,2] Koshi Mimori,[1] Masaaki Iwatsuki,[1] Hideshi Ishii,[1] Ichiro Onoyama,[3] Takeo Fukagawa,[4] Hiroyuki Kuwano,[2] Keiichi I. Nakayama,[3] and Masaki Mori[5]

[1]Department of Surgery, Medical Institute of Bioregulation, Kyushu University, Beppu, Japan; [2]Departments of General Surgical Science, Graduate School of Medicine, Gunma University, Maebashi, Japan; [3]Department of Molecular and Cellular Biology, Medical Institute of Bioregulation, Kyushu University, Fukuoka, Japan; [4]Department of Surgery, National Cancer Center Hospital, Tokyo, Japan; and [5]Department of Gastroenterological Surgery, Graduate School of Medicine, Osaka University, Suita, Japan

Abstract

A molecular target associated with the progression of gastric cancer has not yet been uncovered. *FBXW7* is a tumor suppressor gene transcriptionally controlled by p53 that plays a role in the regulation of cell cycle exit and reentry via c-Myc degradation. Few studies have addressed the clinical significance of *FBXW7* expression in gastric cancer. Therefore, we examined *FBXW7* mRNA expression to determine its clinicopathologic significance in 100 cases of gastric cancer. Low expression levels of *FBXW7* in primary gastric cancer contributed to malignant potential, such as lymph node metastasis ($P = 0.0012$), tumor size ($P = 0.0003$), and poor prognosis ($P = 0.018$). In comparison with 52 cases of gastric cancer without the *p53* mutation, 29 cases with the mutation exhibited lower expression levels of *FBXW7* ($P = 0.0034$), revealing a significant relationship between *p53* mutation and *FBXW7* expression. Furthermore, we found that gastric cancer patients who had low *FBXW7* expression levels and *p53* mutation had a distinctively poor prognosis in comparison with other subgroups ($P = 0.0033$). In conclusion, we showed a role for *p53* in the transcriptional regulation of *FBXW7* expression in clinical gastric cancer cases and showed that disruption of both *p53* and *FBXW7* contributes to poor prognosis. [Cancer Res 2009;69(9):3788–94]

Introduction

FBXW7 is a F-box protein subunit of a SCF-type ubiquitin ligase complex that induces the degradation of positive cell cycle regulators (oncoproteins) such as c-Myc, cyclin E, c-Jun, and Notch. Therefore, *FBXW7* and the associated molecules have been focused on as one of the new carcinoma control structures (1, 2). In particular, *FBXW7* induces cell cycle exit (G_0 phase) via c-Myc degradation, so the altered expression of *FBXW7* is considered one of the major causes of carcinogenesis or carcinoma development (2–4). Because *FBXW7* also participates in cell cycle exit to, and the reentry from, G_0 (5–7), it is a candidate molecular therapeutic target in intractable carcinoma cases that are firmly resistant to combined modality therapies (5, 8).

Mao and colleagues reported that epithelial tumors are not established in $p53^{-/-}$ mice, whereas $p53^{+/-}$ mice form epithelial tumors with altered *FBXW7* expression. *FBXW7* works downstream of *p53*, both of these cell cycle regulator genes, are critical for carcinogenesis of epithelial tissues (3).

Recently, Onoyama and colleagues reported that mice carrying a *FBXW7* T-cell conditional knockout eventually developed thymic lymphomas following thymomas. *FBXW7* and *p53* double-knockout mice developed thymic lymphomas more frequently than other subgroups of knockout mice, such as wild-type, $p53^{-/-}$, and *FBXW7* conditional knockout mice. Therefore, their study clearly showed the consecutive roles of p53 and FBXW7 in the carcinogenesis of solid tumors *in vivo*. Moreover, a comparison of four groups classified according to *FBXW7* and *p53* status revealed a worse prognosis for double inactivation mice than in the other subgroups (6). It is unknown if identical findings were observed during previous *in vivo* studies of human cancer cases.

The clinical significance of *FBXW7* in human solid cancers has been diversely reported. *FBXW7* mutation rates in cholangiocarcinomas, T-cell acute lymphocytic leukemia, endometrial carcinoma, and colorectal cancer were reported as 35%, 31%, 9%, and 9%, respectively (2, 4, 9, 10). Also, *FBXW7* low expression in glioma tissues reportedly produces a poor prognosis (11, 12). Lee and colleagues reported that the *FBXW7* mutation rate in clinical gastric cancer tissues of 3.7% to 6% did not differ in early or progressive gastric cancer (4, 13). However, few studies are available on the connection between *FBXW7* expression level and poor prognoses in gastric cancer.

This study details (*a*) the magnitude of the effect of altered *FBXW7* expression on prognosis determination in gastric cancer cases; (*b*) the significance of both *FBXW7* expression and *p53* mutation status on clinical gastric cancer cases, which was compared with previous *in vivo* reports; and (*c*) how the coexistence of the *p53* mutation and low expression of *FBXW7* in clinical samples determines malignant potential and a poorer prognosis for gastric cancer patients.

Materials and Methods

Clinical samples and cell lines. One hundred gastric cancer samples and paired noncancerous samples were obtained during surgery and used after obtaining informed consent. All patients underwent resection of the primary tumor at Kyushu University Hospital at Beppu and affiliated hospitals between 1992 and 2000. Resected cancer tissues and paired noncancerous tissues were immediately cut and embedded in Tissue-Tek OCT medium (Sakura), frozen in liquid nitrogen, and kept at −80°C until RNA and DNA extraction. Following isolation of RNA and DNA, cDNA was synthesized from 8.0 μg total RNA as described previously (14).

The human gastric cancer cell line AZ521 was provided by the Cell Resource Center of Biomedical Research, Institute of Development, Aging

Note: Supplementary data for this article are available at Cancer Research Online (http://cancerres.aacrjournals.org/).

Requests for reprints: Masaki Mori, Department of Gastroenterological Surgery, Graduate School of Medicine, Osaka University, 2-2 Yamadaoka, Suita 565-0871, Japan. Phone: 81-6-6879-3251; Fax: 81-6-6879-3259; E-mail: mmori@gesurg.med.osaka-u.ac.jp.

doi:10.1158/0008-5472.CAN-08-2846

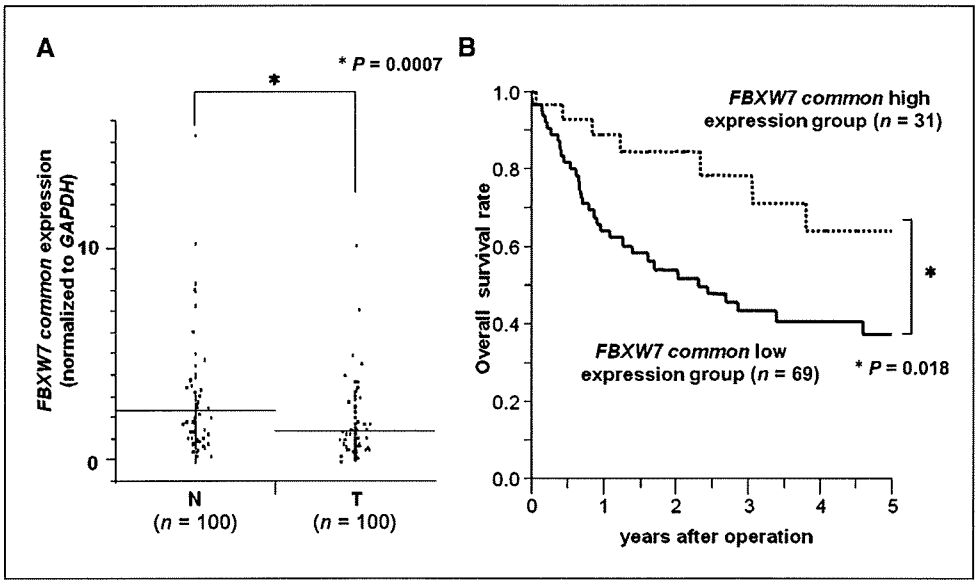

Figure 1. Clinical significance of *FBWX7* mRNA expression in clinical samples. *A*, *FBXW7* mRNA expression in cancer (*T*) and noncancerous (*N*) tissues from gastric cancer patients by real-time reverse transcription-PCR (n = 100). *FBXW7* (T; n = 100), *FBXW7* mRNA (T)/*GAPDH* mRNA (T); *FBXW7* (N; n = 100), *FBXW7* mRNA (N)/*GAPDH* mRNA (N). *Horizontal lines*, mean. *B*, Kaplan-Meier overall survival curves of gastric cancer patients according to the level of *FBXW7* mRNA expression. The high *FBXW7* expression group (n = 31), *FBXW7* (T)/*FBXW7* (N) ≥ 1.0; low *FBXW7* expression group (n = 69), *FBXW7* (T)/*FBXW7* (N) < 1.0.

and Cancer, Tohoku University. This cell line was maintained in RPMI 1640 containing 10% fetal bovine serum with 100 units/mL penicillin and 100 units/mL streptomycin sulfates and cultured in a humidified 5% CO_2 incubator at 37°C.

Real-time quantitative reverse transcription-PCR. *FBXW7*-specific oligonucleotide primers were designed to amplify a 249-bp PCR product encoding the common region among three *FBXW7* isoforms. The following primers were used: *FBXW7* sense primer 5′-AAAGAGTTGTTAGCGGTTCTCG-3′ and antisense primer 5′-CCACATGGATACCATCAAACTG-3′ and glyceraldehyde-3-phosphate dehydrogenase (*GAPDH*; 270 bp) sense primer 5′-GTCAACGGATTTGGTCTGTATT-3′ and antisense primer 5′-AGTCTTCTGGGTGGCAGTGAT-3′. These primers spanned more than two exons to avoid amplification of contaminating genomic DNA. PCR amplification for quantification of *FBXW7* and *GAPDH* mRNA in clinical samples was done in the LightCycler system (Roche Applied Science) using the LightCycler-FastStart DNA Master SYBR Green I Kit (Roche Applied Science) as described previously (15). The amplification conditions of cycles consisted of initial denaturation at 95°C for 10 min followed by 40 cycles of denaturation at 95°C for 10 s, annealing at 62°C (60°C for *GAPDH*) for 10 s, and elongation at 67°C (65°C for *GAPDH*) for 10 s. Melting curve analysis was done to distinguish specific products from nonspecific products and primer dimmers. The relative expression levels of *FBXW7* were obtained by normalizing the amount of *FBXW7* mRNA divided by that of *GAPDH* mRNA as an endogenous control in each sample.

FBXW7 RNA interference. *FBXW7*-specific siRNA (Silencer Predesigned siRNA1: sense GCACAGAAUUGAUACUAACTT and antisense GUUAGUAUCAAUUCUGUGCTG and Silencer Predesigned siRNA2: sense CCUUAUAUGGGCAUACUUCTT and antisense GAAGUAUGCCCAUAUAAGGTG) and negative control siRNA (Silencer Negative Control 1 siRNA) were purchased from Ambion. Lipofectamine RNA interference MAX (Invitrogen) and *FBXW7*-specific siRNA were then added in 6-well flat-bottomed microtiter plates. After incubation, the AZ521 cell line was seeded at 1.5×10^5 per well in a volume of 2 mL in 6-well flat-bottomed microtiter plates and incubated in a humidified atmosphere (37°C and 5% CO_2). The RNA interference assay was done after a 24 h incubation.

Immunoblot analysis. Total protein was extracted from AZ521 after *FBXW7* RNA interference. Aliquots of total protein (35 μg) were electrophoresed in 7.5% concentrated READY GELS J (Bio-Rad Laboratories). c-Myc, cyclin E, and p53 proteins were detected using anti-c-Myc (N-262), anti-cyclin E (M-20), and anti-p53 (Pab240; all obtained from Santa Cruz Biotechnology) diluted 1:500, 1:100, and 1:100, respectively. These proteins were normalized to the level of β-actin protein (Cytoskeleton) diluted 1:1,000. Western blot analysis was done as described previously (16). Enhanced chemiluminescence detection reagents (Amersham Biosciences) were used to detect antigen-antibody reactions.

***In vitro* proliferation assay.** Proliferation was determined using the 3-(4,5-dimethylthiazol-2-yl)-2,5-diphenyltetrazolium bromide assay (Roche Diagnostics). After a 24 h incubation following siRNA addition, cells were cultured further for 0 to 72 h and the absorbance of the samples was measured as described previously (17).

***p53* and *FBXW7* sequence.** Among 100 gastric cancer samples in which *FBXW7* mRNA levels were measured, *p53* was sequenced in 81 genomic DNA samples. Similarly, 80 paired cDNA samples were subjected to *FBXW7* mutational analysis.

The 81 genomic DNA samples were used as templates to PCR amplify exons 4 to 9 of the *p53* gene with primers derived from intronic sequences (Supplementary Table S1). The PCR was done with AmpliTaq Gold DNA Polymerase (Applied Biosystems). Likewise, the *FBXW7* (α, β, and γ) sequence was amplified using cDNA from 80 gastric cancer samples with KOD-FX DNA polymerase (TOYOBO) and sequencing primers (Supplementary Table S1). These PCR products were electrophoresed on 1% agarose gels containing ethidium bromide and purified with ethanol precipitation. Purified PCR products were sequenced using a Big-Dye Terminator version 1.1 Cycle Sequencing Kit (Applied Biosystems) and an ABI3100 sequencer (Applied Biosystems).

Statistical analysis. Differences between two groups were estimated with Student's t test, χ^2 analysis, and ANOVA. Overall survival curves were plotted according to the Kaplan-Meier method, with the log-rank test applied for comparison. Survival was measured from the day of the surgery. Data for *FBXW7* mRNA expression levels in three groups were analyzed with ANOVA. When the results of the ANOVA were significant, Tukey's multiple comparison tests were used to assess differences in *FBXW7* mRNA expression levels among each group. All differences were statistically significant at the level of $P < 0.05$ and a tendency was indicated at the level of $P < 0.1$. Statistical analyses were done using the JMP 5 for Windows software package (SAS Institute).

Results

Clinical significance of *FBXW7* mRNA expression in gastric cancer cases. The expression levels of *FBXW7* mRNA in cancerous tissues (n = 100) and paired noncancerous tissues (n = 100) of the gastric cancer patients were examined by real-time reverse transcription-PCR. These data were corrected for *GAPDH* mRNA levels. *FBXW7* mRNA expression levels in cancer

tissues (mean ± SD, 1.41 ± 1.51) were lower than those in noncancerous tissues (2.37 ± 2.3). A significant difference in mRNA mean expression level was found between cancerous and noncancerous tissues (P = 0.0007; Fig. 1*A*). Immunostaining of FBXW7 was done to confirm the correlation between *FBXW7* mRNA and FBXW7 protein. Fifteen gastric cancer samples were divided into two groups according to FBXW7 protein level (high or low). The expression of *FBXW7* mRNA in each group was examined and compared with protein expression levels. The high FBXW7 protein group (n = 7) showed high *FBXW7* mRNA expression levels in comparison with the low FBXW7 protein group (n = 8; P = 0.0013; Supplementary Fig. S1).

In the overall survival curve (Fig. 1*B*), patients in the low *FBXW7* expression group (n = 69; cancer/noncancerous tissues < 1.0) had a significantly poorer prognosis than those in the high *FBXW7* expression group (n = 31; cancer/noncancerous tissues ≥ 1.0; P = 0.018). However, there was no relationship between *FBXW7* expression and clinical stage progression (Supplementary Fig. S2). Multivariate analysis revealed that the *FBXW7* mRNA expression level in cancer is an independent predictor of lymph node metastasis (Supplementary Table S2*A* and B).

Table 1. *FBXW7* gene expression and clinicopathologic factors for 100 gastric cancer patients

	FBXW7/GAPDH		*P*
	High expression (n = 31)	Low expression (n = 69)	
Age (y)			
≥65	15	30	0.69
<65	16	38	
Gender			
Male	17	49	0.12
Female	14	20	
Histology			
Well, moderate	16	34	0.88
Poor, signet	15	34	
Size (cm)			
<5	22	22	0.0003*
≥5	9	47	
Depth			
T_1 (m, sm)	10	11	0.06†
T_2-T_4 (mp, ss, se, si)	21	58	
Lymph node metastasis			
Absent	18	17	0.0012*
Present	13	52	
Lymphatic invasion			
Absent	12	17	0.15
Present	19	52	
Venous invasion			
Absent	27	45	0.024*
Present	4	24	
Liver metastasis			
Absent	31	65	0.17
Present	0	4	
Peritoneal dissemination			
Absent	30	53	0.014*
Present	1	16	
Stage			
I, II	23	28	0.0019*
III, IV	8	41	

NOTE: High *FBXW7* expression group (n = 31), *FBXW7* (T)/*FBXW7* (N) < 1.0; low *FBXW7* expression group (n = 69), *FBXW7* (T)/*FBXW7* (N) < 1.0. Well, well differentiated; poor, poorly differentiated; moderate, moderately differentiated; signet, signet ring cell.
*P < 0.05.
†P < 0.1.

Clinicopathologic factors were significantly different in the low *FBXW7* expression group (n = 69). There was more progressive tumor size, lymph node metastasis, venous invasion, peritoneal dissemination, and clinical staging compared with the high *FBXW7* expression group (n = 31; P < 0.05). However, no significant differences were observed regarding age, gender, histology, lymphatic invasion, and liver metastasis (Table 1).

Expression of the *FBXW7* isoform and prognosis in gastric cancer cases. In several *in vivo* studies, mouse *Fbxw7* has three isoforms (α, β, and γ). The α isoform is expressed in most tissues, the β isoform is found in the brain and testis, and the γ isoform is in the heart and muscle (5). We confirmed the distribution of *FBXW7* expression in a human panel before searching for *FBXW7* mutations in gastric cancer cases. We found a similar distribution of *FBXW7* mRNA expression between the human panel and laboratory mice (Supplementary Fig. S3). *Fbxw7* γ controls the nucleolar level of c-Myc and cell size and is restricted to muscle cells, which is larger than other cells (5, 18). It has been suggested that *Fbxw7* γ contributes to muscle differentiation through regulation of c-Myc. Therefore, the expression level of *FBXW7* γ in the heart might be very high to regulate heart muscle differentiation (Supplementary Fig. S3).

In addition, the association between overall *FBXW7* expression and poor prognosis was more significant than between the expression of any individual isoform (Supplementary Fig. S4).

***FBXW7* and *p53* mutation analysis.** We examined *p53* mutations in 81 genomic DNA samples and *FBXW7* mutations in 80 cDNA samples, the same paired samples that were used for the *FBXW7* mRNA expression assay. Mutation analysis done with sequencing found *p53* and *FBXW7* mutation rates of 35.8% (29 of 81) and 8.8% (7 of 80), respectively (Fig. 2*A* and *B*; Supplementary Table S3; Supplementary Fig. S5).

Examination of the relationship between *p53* mutation status and *FBXW7* mRNA expression levels revealed that *FBXW7* mRNA mean expression levels in the *p53* mutation (+) group (n = 29; 1.07 ± 1.03) were lower than those in the *p53* mutation (−; n = 52; 1.56 ± 1.79) and noncancerous tissues (n = 100; 2.36 ± 2.3). A significant difference was found between the *p53* mutation (+) group and the other groups (Fig. 3). In addition, no difference was observed between the *p53* mutation (−) gastric cancer tissues and noncancerous tissues.

Mean expression levels of *FBXW7* in the *FBXW7* mutation (+) group (n = 7) were not significantly different from those of the *FBXW7* mutation (−) group (n = 73) and noncancerous tissues (n = 100). The presence of the *FBXW7* mutation was not associated with poor prognosis or clinical stage in gastric cancer patients (Supplementary Fig. S5).

***FBXW7* RNA interference promotes proliferation *in vitro*.** Because *FBXW7* mRNA suppression in cancer tissues is associated with poor prognosis, the protein levels of c-Myc and cyclin E, degradation targets of *FBXW7*, were examined to evaluate *FBXW7* function in gastric cancer cells. *FBXW7*

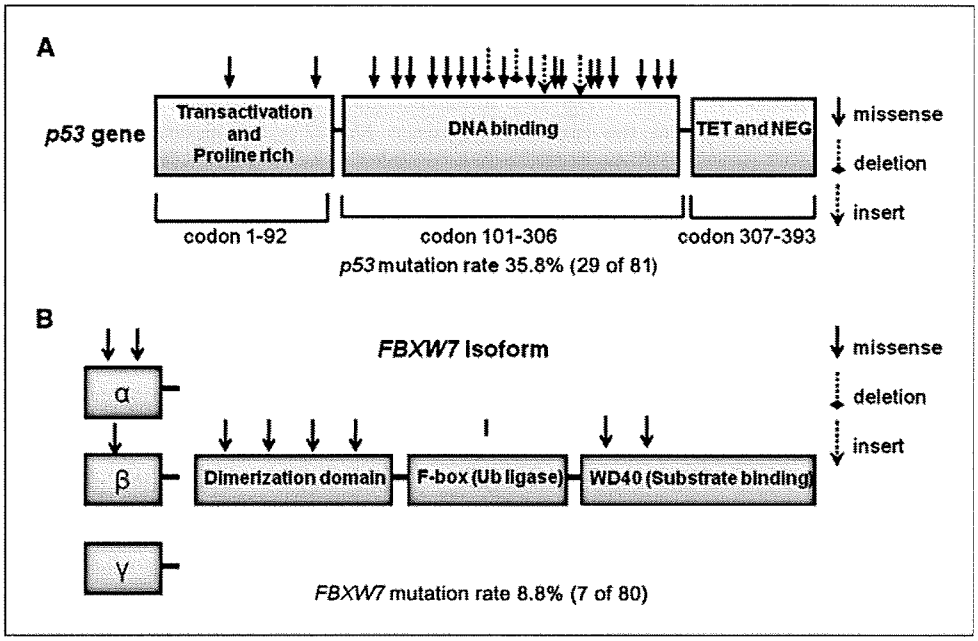

Figure 2. *p53* and *FBXW7* mutation analysis. *A*, structure and mutation of the *p53* gene in gastric cancer patients (n = 81). *B*, structure and mutation of the *FBXW7* gene in gastric cancer patients (n = 80). *Arrows*, mutation type, such as missense, deletion, and insertion.

suppression analysis was done with two different *FBXW7* siRNA (siRNA1 or siRNA2) using gastric cancer cell line AZ521. *FBXW7* suppression by siRNA was confirmed with quantitative reverse transcription-PCR in the control siRNA and *FBXW7* siRNA groups. The level of *FBXW7* mRNA was substantially reduced by 70% in *FBXW7* siRNA1 (Fig. 4*A*).

Western blot analysis confirmed expression of c-Myc and cyclin E proteins degradation targets of *FBXW7* in control siRNA and *FBXW7* siRNA groups. The expression levels of c-Myc and cyclin E protein were enhanced in the *FBXW7* siRNA group compared with the control siRNA group. Likewise, p53 expression was enhanced (Fig. 4*B*). Evaluation of proliferation potency in the *FBXW7* siRNA groups using the 3-(4,5-dimethylthiazol-2-yl)-2,5-diphenyltetrazolium bromide assay showed that proliferation rates were significantly enhanced in both *FBXW7* groups in comparison with the control siRNA group and parent cell line AZ521 (Fig. 4*C*).

***p53* mutation and *FBXW7* expression are associated with poor prognosis in clinical gastric cancer patients.** *FBXW7* mRNA expression was inhibited in *p53* mutation (+) gastric cancer tissues, and the low *FBXW7* expression patients had a significantly poorer prognosis than the high *FBXW7* expression patients (Figs. 1*B* and 3).

Therefore, we divided 81 gastric cancer patients into four groups according to *FBXW7* expression level and the state of the *p53* mutation and examined the overall survival curve in these groups. The *p53* mutation (+), *FBXW7* low expression group (n = 24) had a significantly poorer prognosis than the other three groups (P = 0.0033; Fig. 5).

Discussion

In this study, we showed that *FBXW7* mRNA expression in gastric cancer samples is markedly decreased in comparison with the corresponding noncancerous samples and that *FBXW7* is a poor prognostic factor. There are three possible explanations. First, it is worth noting that *FBXW7* expression is regulated by p53 in *in vitro* and *in vivo* experimental data (3, 5, 6, 19). For instance, Mao and colleagues reported that *Fbxw7* mRNA expression was activated when *p53* expression was induced by radiation, and baseline expression of *Fbxw7* mRNA is suppressed in $p53^{-/-}$ mice. Moreover, they reported that a p53-binding site is present in a promoter region of the mouse *Fbxw7* (3). In addition, Kimura and colleagues reported that *FBXW7* β expression is enhanced when wild-type *p53* is produced in a *p53*-mutated glioblastoma cell line (8). These reports strongly suggest that transcription of *FBXW7* is regulated by p53 activity. Therefore, we focused on the regulation of *FBXW7* expression by p53 in gastric cancer cases. In the current study, *FBXW7* expression levels were decreased in most *p53* mutation (+) gastric cancer samples (Fig. 3); only 6% (5 of 81) cases were *FBXW7* high expression in *p53* mutation (+; Fig. 5). Most of the p53 mutation (+) gastric cancer patients belonged to the *FBXW7* low expression group. Therefore, we propose that *FBXW7* mRNA expression is primarily regulated by the presence of the *p53* mutation in clinical gastric cancer cases. It is worth noting that the reproducibility of this finding *in vivo* was clearly confirmed in human clinical cases. To determine which isoform of *FBXW7* is regulated by p53 *in vitro*, we used *p53* siRNA to suppress *p53* expression in gastric cancer cell line AZ521. The expression levels of the three *FBXW7* isoforms (α, β, and γ) were suppressed by *p53* siRNA (Supplementary Fig. S6).

Second, we determined that *FBXW7* is inactivated by a mutation in the coding region. The average of *FBXW7* mutation rate in several malignancies was ~6% (4). As for gastric cancer cases, Lee and colleagues reported the possibility of the presence of mutation, but the relationship of the *FBXW7* mutation and prognosis was not elucidated (13). Therefore, we examined the sequence of the *FBXW7* isoforms. The *FBXW7* mutation rate, 8.8% (7 of 80), was similar to the 3.7% to 6% previously reported for gastric cancer (4, 13). Mutation hotspots are located in T-cell acute lymphocytic leukemia; however, they were not detected in the current study (13, 20, 21).